JPRS-CST-91-011
31 MAY 1991

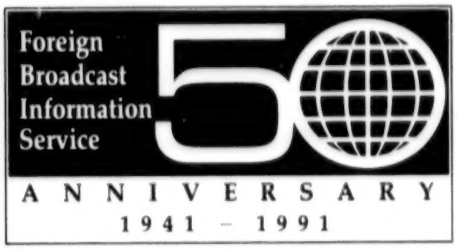

JPRS Report

Science & Technology

China

Science & Technology
China

JPRS-CST-91-011 31 May 1991

CONTENTS

AEROSPACE

China To Promote Satellite Technology *[Li Hong; CHINA DAILY, 23 Apr 91]* 1

DEFENSE R&D

Megawatt-Level 8-mm Relativistic Orotron, 3-cm Relativistic Backward-Wave Tube Developed
[Deng Xianchun; ZHONGGUO KEXUE BAO, 1 Mar 91] 2
Analysis and Numerical Results of Complex-Cavity Gyrotron
[Li Hongfu, Meng Lin; DIANZI XUEBAO, Mar 91] 2
State-Run Plant 740's Export Electron Tubes Meet Varian's EIMAC Quality Standard
[Ren Jiliang, Qi Xuanjiang; ZHONGGUO DIANZI BAO, 17 Mar 91] 2
Theoretical Studies of Reflection and Diffraction of EM Wave by Grating
[Yang Rongsheng, Guo Kaizhou, et al.; DIANZI KEXUE XUEKAN, No 2, Mar 91] 2

BIOTECHNOLOGY

Status of Biotechnology Development Reviewed *[Hou Yunde; ZHONGGUO KEJI LUNTAN, Jan 91]* .. 4
Nd: YAG Laser Iridotomy for Angle-Closure Glaucoma
[Li Jingzhen, Zhang Chengfen, et al.; ZHONGHUA YANKE ZAZHI, Jan 91] 5
High Level Expression of a Segment of HIV-1 env Gene in E. coli
[Wu Weixing, Ma Xiankai; ZHONGHUA WEISHENGWUXUE HE MIANYIXUE ZAZHI, No 1, Feb 91] 5
Nucleotide and Encoded Amino Acid Sequences of the Nonstructural Protein NS1 Gene of a Dengue-2 Virus Isolated in China
[Yang Peiying, et al.; ZHONGHUA WEISHENGWUXUE HE MIANYIXUE ZAZHI, No 1, Feb 91] 5
Genetically-Engineered Hemorrhagic Fever Vaccine
[Wang Jingzhu; YIYAO XINXI LUNTAN, 28 Mar 91] 6
Inhibitory Action of Venom of Agkistrodon Halys Pallas From Zhejiang Province on Platelet Aggregation and Release of Adenosine Nucleotide
[Bao Chengxin; ZHONGHUA XUEYEXUE ZAZHI, No 2, Feb 91] 6
Hydrophobic Modification of Water Soluble Drug and Its Reconstitutable Liposomes
[Hou Xinpu, et al.; YAOXUE XUEBAO, Nov 90] 6
Synthesis of 2-Formyl (Acetyl) Substituted Quinoline Thiosemicarbazones
[Wang Rui, Leng Zongkang, et al.; YAOXUE XUEBAO, Dec 90] 6
Purification and Biochemical, Pharmacological Characteristics of an Acidic Phospholipase A_2 of Ophiophagus hannah Venom From Fujian
[Huang Minzhou, Liu Guangfen, et al.; SHENGWUHUAXUE YU SHENGWUWULI XUEBAO, No 1, Jan 91] 7
Purification and Characterization of Cobra Venom Factor (CVF) From Chinese Cobra (Naja naja atra)
[Shu Yuyan, Zhuang Maoxin, et al.; SHENGWUHUAXUE YU SHENGWUWULI XUEBAO, Jan 91] . 7
Synthesis of Peptide T—A Comparison Study
[Wu Tongde, Chu Jiyu, et al.; HUAXUE XUEBAO, Nov 90] 7
Cloning and Expression of Polyhedrin Gene From Insect Virus in E. coli Cell
[Qi Yipeng, Huang Yongxiu, et al.; WEISHENGWU XUEBAO, No 1, Feb 91] 7
Cloning and Expression of Streptomyces lividans Promoters
[Huan Liandong, Dong Kening, et al.; YICHUAN XUEBAO, No 1, Feb 91] 8
Molecular Cloning of Lipopolysaccharide Genes of the Vibrio Cholerae in E. coli HB101
[Shao Huang, Ma Qingjun; WEISHENGWU XUEBAO, No 1, Feb 91] 8
Nitrogen-Fixation Research Project Bears Fruit *[Zhang Xuequan; RENMIN RIBAO, 27 Feb 91]* 8

COMPUTERS

Four Convex C120 Minisupercomputers Receive U.S. Commerce Department License for Export to China *[JISUANJI SHIJIE, 27 Mar 91]* 9

FACTORY AUTOMATION, ROBOTICS

On Implementing Chinese-Style CIM (Part II) *[Li Kaifo; JICHUANG, Jan 91]* 10

LASERS, SENSORS, OPTICS

New Technique for Laser U-Isotope Separation Passes Feasibility Appraisal
[Fu Ke; KEJI RIBAO, 2 Mar 91] 15
Krypton-Fluoride Excimer Laser Debuts *[Peng Dejian; ZHONGGUO KEXUE BAO, 22 Mar 91]* 15
Experimental Coherent CW-CO_2 Laser Imaging System
[Fan Liming, Nan Jingda, et al.; GUANGXUE XUEBAO, Dec 90] 15
Free Electron Laser With Grazing Incidence Ring Resonator
[Wang Mingchang, Yuan Youlong, et al.; GUANGXUE XUEBAO, Dec 90] 17
Microwave Emission from a Virtual Cathode Source
[Wang Pingshan, Hu Kesong; QIANG JIGUANG YU LIZI SHU, Aug 90] 20
X-Ray Laser Gain Measurements, Beam Optics Diagnostics in Ne-Like Ge
[He Shaotang, He An, et al; WULI XUEBAO, Nov 90] 21
Designing Large Digital Sonar System Using Cascade Link Array Processors
[Liu Qiushi, Li Shicai, et al; SHENGXUE XUEBAO, May 90] 22
Pulsed Slab Nd:YAG Laser *[Gong Mali, Han Kai, et al.; ZHONGGUO JIGUANG, Jan 91]* 28
New CCD Image-Pickup Camera Developed *[Yu Ruming; ZHONGGUO DIANZI BAO, 1 Mar 91]* 30
Evolution From Periodicity to Non-Periodicity of Electron Phase Orbits in Free-Electron Laser with Untapered Wiggler *[Zhang Shichang, Hu Zhongxiu, et al; WULI XUEBAO, Nov 90]* 30
Threshold Conditions for Pulsed Laser-Induced Spallation in Metals
[Sun Chengwei, Zhuang Shiming; QIANG JIGUANG YU LIZI SHU, Aug 90] 31
Numerical Simulations of Laser Ignition of PETN and Interactions of Explosion Waves with Al Targets
[Zhang Zhongzheng, Duan Zhuping; QIANG JIGUANG YU LIZI SHU] 31

SUPERCONDUCTIVITY

Four Devices Developed by MMEI's Institute 16 Pass Technical Appraisal
[Wang Huizhi; DIWEN YU CHAODAO, No 1, Feb 91] 32
Influence of Coupling Network on Noise, Frequency Response of DC SQUID Magnetometer
[Zhang Lihua, Weng Yaojun, et al.; DIWEN YU CHAODAO, No 1, Feb 91] 32
Effect of Doping Ag on Superconducting Properties of TlBaCaCuO System
[Li Chengen, Zhao Meiyu, et al; GUISUANYAN XUEBAO, No 1, Feb 91] 33
Optimum Percentage of Pb and Appropriate Thermal Procedure for Preparation of 110K $Bi_{2-x}Pb_xSr_2Ca_2Cu_3O_y$ Superconductor *[Wan Fabao, et al.; DIWEN YU CHAODAO, No 1, Feb 91]* .. 33
rf-SQUID and the Grain Property of YBCO
[Lin Dong, Yang Tao,et al.; DIWEN YU CHAODAO, No 1, Feb 91] 33
In-Situ Deposition of YBCO Superconducting Thin Films by Laser Ablation
[Zhang Yaogang, Shi Changqing, et al.; DIWEN YU CHAODAO, No 1, Feb 91] 34

China To Promote Satellite Technology

40100043A Beijing CHINA DAILY in English 23 Apr 91 p 1

[Article by staff reporter Li Hong]

[Text] China aims to push forward the application of satellite technology in the next 10 years to enhance the country's economic and defence capabilities.

While China still lagged behind advanced countries in developing and using satellites, it had achieved considerable success from a series of satellites launched in recent years which have proved instrumental to economic development, an official from the Ministry of Aeronautics and Astronautics Industry told CHINA DAILY.

The official said the country was to intensify its efforts in developing six satellite systems in the last decade of this century.

They were a telecommunication and broadcasting system, air communication control system, disaster prevention system, environmental protection and resource-detecting system, space research system and defence system.

But the official declined to give details of what and how many satellites the country planned to develop.

China is now busy producing a large-capacity 24-transponder communication satellite—the "Dongfanghong 3"—which is capable of covering all of China's land area.

It is also doing research on a satellite weather forecasting network, and is manufacturing a resource satellite in collaboration with Brazil.

The official pointed out that China still lagged behind the Soviet Union and the United States in developing and using satellites.

China has developed only five types of applicable satellite, compared with the 27 developed throughout the world.

But the official said the telecommunication, weather and retrievable remote-sensing satellites developed by Chinese scientists had brought enormous benefits to other sectors of the economy.

The four telecommunication satellites developed and sent into space since 1986 were now capable of transmitting TV and radio programmmes from Beijing to all parts of the country and even abroad, the official said.

The official said transmission of TV training courses, made possible by the satellites, had saved China about 5 billion yuan ($960 million) a year.

And timely information relayed from China's weather satellite had reduced losses from typhoons, floods, fires and other disasters.

The Fengyun-1 satellite sent to space last September, the official said, was believed to be capable of monitoring all typhoons in the northwestern Pacific area.

The United States, Australia, Pakistan, Hong Kong and Taiwan were regularly using data provided by the satellite.

Meanwhile, 12 retrievable remote-sensing satellites had helped China to detect large coal deposits in the Inner Mongolia Autonomous Region and an oilfield in Northwest China's Xinjiang Uygur Autonomous Region.

Megawatt-Level 8-mm Relativistic Orotron, 3-cm Relativistic Backward-Wave Tube Developed

91P60169A Beijing ZHONGGUO KEXUE BAO [CHINESE SCIENCE NEWS] in Chinese 1 Mar 91 p 2

[Article by Deng Xianchun [6772 6343 2504]: "Chengdu University of Electronic Science and Technology Is First To Develop 8-mm Relativistic Orotron, 3-cm Relativistic Backward-Wave Tube"]

[Summary] Chengdu—A Chengdu University of Electronic Science and Technology High-Energy Institute research team led by institute associate director and associate research fellow Yu Shanfu [0060 0810 1133] and by associate research fellow Li Jiayin [2621 1367 5255] has recently developed an 8-mm-wavelength relativistic orotron and a 3-cm-wavelength relativistic backward-wave tube (BWT). In their work on the orotron, the researchers for the first time domestically developed an impedance-matched dual-cathode cold-cathode electron gun, employed a radiation field to measure cavity modes, resolved problems associated with fabrication of a corrugated-waveguide cavity, and developed a high-quality, high-performance dynamic-state vacuum chamber and pulse magnetic field. Employing a high-density pulse accelerator as the energy source, this 8-mm relativistic orotron can generate up to 6 megawatts of microwave radiation.

In their work on the 3-cm relativistic BWT, the researchers improved the centering between the pulse magnetic field and the system, constructed a 3-cm waveguide dispersion line, and resolved problems associated with fabrication of a 3-cm corrugated-waveguide slow-wave line. The relativistic BWT's [output] power can reach 90 megawatts, with an efficiency of about 10 percent.

Analysis and Numerical Results of Complex-Cavity Gyrotron

40100048 Beijing DIANZI XUEBAO [ACTA ELECTRONICA SINICA] in Chinese Vol 19 No 2, Mar 91 pp 8-12, 38

[English abstract of article by Li Hongfu and Meng Lin of the University of Electronic Science and Technology of China. (MS received Sep 89, revised Aug 90)]

[Text] A complex-cavity gyrotron is analyzed and calculations are given. The resonance frequency, Q-value and field-profile function are solved numerically. On the basis of this, large-signal analysis of it is carried out. The relation between the interaction efficiency and some parameters is investigated in the case of the interaction of the fundamental wave with the secondary electron harmonic. The results show that the complex-cavity may operate in a high-order mode, and provide a very high output power and rather high interaction efficiency by appropriate design of the complex-cavity structure.

State-Run Plant 740's Export Electron Tubes Meet Varian's EIMAC Quality Standard

91P60169B Beijing ZHONGGUO DIANZI BAO [CHINA ELECTRONICS NEWS] in Chinese 17 Mar 91 p 2

[Article by Ren Jiliang [0117 4949 5328] and Qi Xuanjiang [7871 3763 3068]: "Visit With State-Run Plant 740's Quality Control Manager Is a Fruitful Experience"]

[Summary] Last year, a joint group representing the REL Co., the world's largest commercial distributor of electron tubes, and the Varian Co., a first-rate manufacturer of electron tubes, conducted an on-site acceptance check of the export products manufactured by State-Run Plant 740. The acceptance-check team included QC specialists from Varian's EIMAC plant. After a number of rigorous tests, the QC specialists certified a series of seven electron-tube export products (4CX250B, 4CX350A, 4CX350F, 8560A, 4CX1000, 4CX5000A, and 4CX10000D) manufactured by Plant 740 as fully complying with EIMAC quality standards, and agreed that the products could bear the EIMAC trademark for sale on the international market.

EIMAC standards are quite rigorous, and satisfy U.S. milspec requirements. Plant 740 has imported from the United States 137 items of 1980's-era advanced technology—including instruments with 1-micron accuracy—and has sent over 40 engineers and technicians to the United States for specialized training.

Last year, following the granting of permission for Plant 740's use of the EIMAC trademark, the foreign exchange earned broke through the US$1 million mark. Moreover, the 4CX250B metal-ceramic transmitting tube has been awarded a State Quality Award.

Theoretical Studies of Reflection and Diffraction of EM Wave by Grating

40100045A Beijing DIANZI KEXUE XUEKAN [JOURNAL OF ELECTRONICS] in Chinese Vol 13 No 2, Mar 91 pp 119-124

[English abstract of article by Yang Rongsheng, Guo Kaizhou, and Song Wenmiao of the Institute of Electronics, CAS, Beijing; MS received 21 Nov 89, revised 22 Mar 90]

[Text] The electromagnetic field problem of a rectangular grating illuminated with TM wave is studied theoretically by means of rigorous field-matching and moment method. The numerical calculations show that the grating, as a frequency-scan antenna, can produce perfect blazing in a wide range of incident angle only through adjusting the size of width and depth of the

groove no matter whether the Bragg condition is satisfied or not. Higher efficiency and broader frequency band of -1 order diffraction wave can be achieved only at the larger reciprocal incident angle. And a very broad frequency band can be expected when the grating is employed as a reflecting mirror in an orotron. The effective grating position and phase change of reflection wave by grating are also numerically presented.

Status of Biotechnology Development Reviewed

91P60162 Beijing ZHONGGUO KEJI LUNTAN [FORUM ON SCIENCE AND TECHNOLOGY IN CHINA] in Chinese No 1 Jan 91 pp 57-59

[Article by Hou Yunde [0186 0061 1795], Chief Scientist of the '863 Plan' Biotechnology Expert Committee; "Present Situation of Biotechnology Development in China"]

[Excerpts] [Passage omitted] As a developing country with a population of 1.1 billion, China's national economy lies in agriculture. Therefore, the overall strategy for national economic development should be quadrupling the industrial and agricultural GNP by the end of 21st Century through biotechnology application in promoting agricultural and medicinal progress. China's plan to develop biotechnology is: 1) Place biotechnology development plan on top of other high technology development plans to improve agricultural production of grains, fertilizer, and livestock; 2) Put priority on biotechnologically developed new products in agriculture, forestry, animal husbandry, fishery, medicine, health, light industry and foodstuffs. Focus key research projects on agriculture, quickly form a high technology production system and give priority to the production of urgently-needed, technology-mature or high economic and social return products. The production of genetically engineered hepatitis B vaccine for the 100 million HBV carriers is a good example; 3) Accelerate technology innovation in conventional industries to promote technology standards and improve product quality and variety. China should combine new and conventional technologies in screening high-quality varieties, develop high-yield fermentation devices that can be used for culturing either bacteria or mammalian cells and the purification-monitoring-analysis devices for protein and nucleic acid products, and actively apply new enzyme engineering and fermentation engineering technology for conventional industries' technology reforms; 4) Vigorously promote biotechnology development because of the urgent demand and weak research-production linkage in China. China should establish crucial technology systems, such as bioreactor systems, to promote transformation of S&T achievements to production; 5) Pay more attention to basic research in biotechnology and related areas; 6) Establish necessary basic facilities for biotechnology development, for example, the establishment of purification systems for separating restriction endonuclease and other modifying enzymes, isotopes and proteins, and the production systems for supplying cell-culture media, and the establishment of cell library, genomic library, and biotechnology data base; 7) Strengthen international academic exchange, technology cooperation and technology import by establishing national key laboratories equipped with advanced facilities in order to attract foreign technologies that are already mature abroad and are urgently needed in China; 8) Establish biotechnology legislation system to avoid unnecessary side effects from biotechnology development, especially those derived from producing recombinant DNA; and 9) Strengthen management and coordination in biotechnology R&D. Although biotechnology is a part of the '863' Plan and is directly under the administration of the State Science Commission, the actual administrative work is carried out by the State Biotechnology Development Center established in 1983. The Biotechnology Expert Committee, composed of 10 top scientists selected from the research institutes all over the country by the State Science Commission, is the main body to formulate biotechnology strategy, to ensure the implementation of special research projects and sources of funds for these projects. The Expert Committee is also responsible for monitoring and promoting cooperation between research institutes and production units to accelerate new products development and production.

Focal Points of Biotechnology Research:

(1) Produce new, high-yield, disease-resistant animals, hybrid rice, transgenic plants, high-nutrition grains, test-tube calves, transgenic fishes and livestock; locate rice genes; conduct tests on symbiotic or combined nitrogen fixation.

(2) Produce new drugs, vaccines, genetic-engineered vaccines for gene therapy, polypeptide drugs for treating infectious diseases, malignant tumors, and cardiovascular diseases; focus on antibody engineering and guided-drugs research, protein separation and purification technology, and gene-therapy research.

(3) Emphasize protein engineering research in producing insulin, trichosanthin, urokinase, trypsin, proteinase inhibitors, and subtilin.

The Most Prominent Achievements Are:

(1) Some important target products having economic and social benefits, such as two-line hybrid rice, high nitrogen-fixation soybean root-nodule bacteria, rice-corn combination nitrogen-fixation, test-tube calves, have attained international advanced levels; a new technology to produce genetic-engineered hepatitis B vaccine using microvector technique has been established; and eight new drugs have been developed.

(2) Basically, China has mastered most of the leading-edge technology, especially in plant biotechnology; more progress has been made in light/temperature-sensitive nuclear sterile gene.

(3) With limited funds, three joint research development centers were established to carry out intermediate tests of '863' target products, such as genetic-engineered hepatitis B vaccine, interferon and interleukin-2, and to speed up development of more high-technology products.

(4) Management of the Expert Committee has been improved, a series of administrative regulations for

bringing the '863' plan's results onto the international market have been formulated.

(5) Attraction of a group of 1500 young scientists to form high-tech R&D team.

Problems Encountered in Developing China's Biotechnology:

(1) Lower-stream processing capability of genetically-engineered products is far below the international level;

(2) Only a few basic research areas reach the international level, most of the applied research areas are copies of western research;

(3) Supplies of chemical reagents and disposable laboratory equipment are very limited. Most of the essential reagents for biotechnology research are imported from abroad using hard currency;

(4) An estimated 5,000 Chinese scientists and students are still abroad, half of them in the United States.

(5) Goals of biotechnology development between developing countries and developed countries are different, however there is little cooperation between Chinese scientists and those of other developing countries.

Nd: YAG Laser Iridotomy for Angle-Closure Glaucoma

40091009F Beijing ZHONGHUA YANKE ZAZHI [CHINESE JOURNAL OF OPHTHALMOLOGY] in Chinese Vol 27 No 1, Jan 91 pp 30-33

[English abstract of article by Li Jingzhen [2621 7234 6297], Zhang Chengfen [1728 2110 5358], et al., of the Eye Research Center, PUMC Hospital, Beijing]

[Text] Fifty-six eyes of primary angle-closure glaucoma were performed peripheral iridotomy with the domestic JYZ-1 Model YAG laser microruptor. The success rate was 100 percent. On the average, the number of laser shots was 5 (3.6-31) times, the shot energy was 212 (171-961) mJ, and the follow-up was 3.57 months. Postoperatively, the IOP [intraocular pressure] was lowered by 2.43 mmHg, the use of hypotensive drugs diminished, and the index of chamber angle closure improved. The immediate operative complications were IOP elevation, iris bleeding, and anterior uveitis, which responded well to treatment.

High Level Expression of a Segment of HIV-1 env Gene in E. coli

40091008A Beijing ZHONGHUA WEISHENGWUXUE HE MIANYIXUE ZAZHI [CHINESE JOURNAL OF MICROBIOLOGY AND IMMUNOLOGY] in Chinese Vol 11 No 1, Feb 91 pp 1-4

[English abstract of article by Wu Weixing [0702 5898 2502] and Ma Xiankai [7456 6343 0418] of the Institute of Basic Medical Science, Academy of Military Medical Sciences, Beijing]

[Text] A segment of HIV-1 env gene, covering 540 to 639 amino acids of the transmembrane protein gp41, was cloned on pEx31, and the truncated env protein was expressed in MS_2-env fused polypeptide under the control of P_L promoter in E. coli. This represents about 20 percent of total bacterial proteins. Western blot analysis showed that the expressed products could be recognized by the specific anti-gp41 antibody in AIDS patient's serum. This is the first demonstration of high level expression of HIV env gene in E. coli in China. The significance of the expressed recombinant env protein was discussed.

Nucleotide and Encoded Amino Acid Sequences of the Nonstructural Protein NS1 Gene of a Dengue-2 Virus Isolated in China

40091008B Beijing ZHONGHUA WEISHENGWUXUE HE MIANYIXUE ZAZHI [CHINESE JOURNAL OF MICROBIOLOGY AND IMMUNOLOGY] in Chinese Vol 11 No 1, Feb 91 pp 9-12

[English abstract of article by Yang Peiying [2799 0160 5391] of the Department of Virology, Institute of Microbiology and Epidemiology, Academy of Military Medical Science, Beijing, and I. M. Kautner, et al. of the Department of Microbiology, University of Malaya]

[Text] We report here the nucleotide and encoded amino acid sequences of the NS1 gene of a dengue-2 (DEN-2) virus, strain D_2-04, isolated in 1985 from a patient in Hainan, China. The sequences were then compared with the corresponding sequences from dengue-1 (DEN-1), dengue-4 (DEN-4), and other DEN-2 viruses, the prototype New Guinea C (NGC) virus, the Jamaica (JAM) strain 1409, the candidate vaccine strain S1 (S1) and a Malaysia isolate, M3, isolated from a patient with dengue fever.

The NS1 gene contains 1056 nucleotides with a base composition of 33.6 percent A, 20.6 percent C, 24.5 percent G, 21.2 percent U and encoded a polypeptide of 352 amino acid. The polypeptide contained 1) two potential N-linked glycosylation sites at amino acid residues 130 and 207; 12 conseved cysteine residues did not change, six of which were located within a 50 amino acid stretched from residues 280-330; 3) one possible cleavage site with the consensus sequence "Val (x) Ala at residues 350-352. [quotation marks as published] The sequences compared with corresponding sequences from DEN-2. NGC, JAM, S1 Malaya M3, DEN-1 and DEN-4 reveals homologies of 90.8, 93.5, 89.8, 87.8, 68.1 and 65.7 percent, respectively. The similarity of amino acid is 92.3, 93.4, 92.8, 90.6, 70.5, 69 percent, respectively. The nucleotide changes were scattered throughout the gene but occurred mostly in the third position of the codons. Therefore the degree of similarity was higher at the amino acid level than the nucleotide level.

Genetically-Engineered Hemorrhagic Fever Vaccine

91P60167A Beijing YIYAO XINXI LUNTAN [CHINA MEDICAL TRIBUNE] in Chinese 28 Mar 91 p 1

[Article by Wang Jingzhu [3769 2533 3796]]

[Summary] A research group led by Hang Changshou of the Virology Institute, Chinese Academy of Preventive Medicine, has achieved expression of Hantan (Apodemus agrarius) type M-segment viral gene. The genetically engineered Hantan-type M-segment viral gene, the main gene site to produce neutralizing antigens, was transferred to mammalian cells through expression vectors in order to express the antigen-producing gene in mammalian cells. The protective antigen (genetically-engineered polypeptide vaccine) obtained from mammalian cells was then transferred to vaccinia virus by transinfection. A recombinant vaccinia virus expressing the transinfected gene was thus established. McAb Immunofluorescence Assay, ELISA and Immuno-Electroscopic Assay used to test gene expressions prove that the obtained recombinant vaccinia virus may be used as a live vaccine to produce hemorrhagic fever antibodies.

Inhibitory Action of Venom of Agkistrodon Halys Pallas From Zhejiang Province on Platelet Aggregation and Release of Adenosine Nucleotide

40091009G Tianjin ZHONGHUA XUEYEXUE ZAZHI [CHINESE JOURNAL OF HEMATOLOGY] in Chinese Vol 12 No 2, Feb 91 pp 73-74, 111

[English abstract of article by Bao Chengxin [0545 2110 9515] of the Institute of Hematology, CAMS Tianjin]

[Text] Effect of ZJAV (Venom of Agkistrodon Halys Pallas from Zhejiang Province) on platelet functions was observed in vitro. Inhibitory action of ZJAV on platelet aggregation and release of adenosine nucleotide induced by ADP (2 μmol/L), collagen (10 mg/l) and ristocetin (1.5 g/l) was dose-dependent. In 10 mg/L of ZJAV concentration, platelet agglutination and release of adenosine nucleotide induced by ristocetin could be completely inhibited, but not inhibited when induced by ADP or collagen.

The response of platelet agglutination to ristocetin was restored when platelets were preincubated with ZJAV at 37°C for 3 min and were resuspended into autogenous PPP [poor-platelet plasma]. Platelets binding with McAb AN 51 were unaffected after treatment of ZJAV. These results showed that the mechanism of ZJAV on ristocetin-induced agglutination had relation with both plasma factor and release of adenosine nucleotide from platelet.

Hydrophobic Modification of Water Soluble Drug and Its Reconstitutable Liposomes

40091010A Beijing YAOXUE XUEBAO [ACTA PHARMACEUTICA SINICA] in Chinese Vol 25 No 11, Nov 90 pp 854-858

[English abstract of article by Hou Xinpu [0186 2450 2613], Cui Donghui [1508 2639 6540], et al., of the School of Pharmacy, Beijing Medical University, Beijing 100083]

[Text] Water soluble drugs carried in liposomes have rather low encapsulation percentage (EP%) and poor stability. In this paper metronidazole (I) was chosen as a model of water soluble drugs which was modified by means of esterification. Its myristic ester (II) was synthesized. On studying the liposomes of I and II, the results have shown that EP% and stability of II were more than ten times as high as that of I. Furthermore, the reconstitutable liposomes of II were prepared successfully. The amoebacide activity of II liposomes was increased also. Therefore, the hydrophobic modification of water soluble drugs is a good way to improve the drug entrapped in liposomes.

Synthesis of 2-Formyl (Acetyl) Substituted Quinoline Thiosemicarbazones

40091010B Beijing YAOXUE XUEBAO [ACTA PHARMACEUTICA SINICA] in Chinese Vol 25 No 12, Dec 90 pp 920-925

[English abstract of article by Wang Rui [3769 6904], Leng Zongkang [0397 1350 1660], et al., of the Nanjing Institute of Materia Medica, Nanjing 210009]

[Text] A series of 2-formyl (acetyl) substituted quinoline thiosemicarbazones (III, XII, XIII) were prepared in order to evaluate their antimalarial activity. Oxidation of substituted quinolines (IV) with selenium dioxide gave 2-formyl substituted quinolines (V). 2-Acetyl substituted quinoline (IX) was obtained from IV by oxidation, esterification, Claisen condensation and decarboxylation. III_{1-9} were synthesized by two methods; one was by condensation of 2-formyl (acetyl) substituted quinolines with methyl hydrazinecarbodithioate to form methyl-3-[1-(2-quinolinyl)-alkylidene] hydrazinecarbodithioate (XI), then the S-methyl group of XI was displaced by substitute amines to form the desired substituted thiosemicarbazones. The other was by condensation of 2-formyl (acetyl) substituted quinolines with 4-substituted-3-thiosemicarbazide (X) to afford directly III_{1-9}. III_{10-12} were obtained by selective reduction of corresponding nitro compounds with stannous chloride and XII as a by-product was obtained by the nonselective reduction of III_7 with stannous chloride. 3-Hexyl-4-oxothiazolin-2-yl (2-formyl or acetyl substituted quinoline) hydrazones ($XIII_{1,2}$) were prepared from $III_{1,4}$ via cyclization under sodium acetate condition.

Eighteen compounds were found to be inactive in mice infected with ANKA strain of Plasmodium berghei.

Key words: Antimalarial; 2-Formyl (Acetyl) substituted quinoline; Thiosemicarbazones.

Purification and Biochemical, Pharmacological Characteristics of an Acidic Phospholipase A_2 of Ophiophagus hannah Venom From Fujian

40091009B Shanghai SHENGWUHUAXUE YU SHENGWUWULI XUEBAO [ACTA BIOCHIMICA ET BIOPHYSICA SINICA] in Chinese Vol 23 No 1, Jan 91 pp 70-77

[English abstract of article by Huang Minzhou [7806 2404 1558], Liu Guangfen [0491 1639 5358], et al., of the Laboratory of Venoms Research, Department of Pharmacology, Fujian Medical College, Fuzhou]

[Text] An acidic phospholipase A_2 was isolated and purified from the venom of Ophiophagus hannah by CM-Sephadex C-50 ion-exchange column chromatography and gel filtration on Sephadex G-50. It is homogenous as demonstrated by pH 4.3 PAGE, pH 8.9 SDS-PAGE and isoelectrofocusing electrophoresis. It shows the following characteristics: contains a total of 92 amino acid residues (Trp and Cys were not determined); molecular weight, 13000d; isoelectric point, 5.7; PLA_2 activity, 23 μmol/mg x min; optimal pH, 8.5; optimal temperature, 65°C; LD_{50} (iv, in mice), 3.6 (2.73-4.75) mg/kg. It showed an apparent inhibitory effect on rabbit platelet aggregation and cardiotoxic action on isolated rat hearts, but did not exhibit anticoagulant activity on rabbit plasma.

Purification and Characterization of Cobra Venom Factor (CVF) From Chinese Cobra (Naja naja atra)

40091009A Shanghai SHENGWUHUAXUE YU SHENGWUWULI XUEBAO [ACTA BIOCHIMICA ET BIOPHYSICA SINICA] in Chinese Vol 23 No 1, Jan 91 pp 32-39

[English abstract of article by Shu Yuyan [5289 7183 7159], Zhuang Maoxin [8369 5399 6580], et al., of the Department of Biochemistry, Guangxi Medical College, Snake Venom Research Institute of Guangxi Medical College, Nanning; project supported by the National Natural Science Foundation of China]

[Text] An anticomplement factor, cobra venom factor (CVF), from the venom of Chinese cobra (Naja naja atra) was purified by ion-exchange chromatography on DEAE-Sepharose CL-6B, CM-Sepharose CL-6B, and repurified on hydroxyapatite. The purified CVF was shown to be homogeneous in discontinuous polyacrylamide gel slab electrophoresis. Its molecular weight was estimated to be about 227000-230000 by gradient polyacrylamide gel PAA 4/30 and high performance liquid chromatography (HPLC), and to be 237000 by SDS-polyacrylamide gel electrophoresis. The isoelectric point was about 6.2. SDS-polyacrylamide gel electrophoresis in the presence of dithiothreitol indicated that CVF might consist of three different kinds of polypeptide chains linked by disulfide bridges. All subunits were shown to be glycoproteins when stained with Coomassie brilliant blue R-250 and periodate-Schiff's reagent. CVF contained 2.21 percent neutral hexose and 0.61 percent sialic acid and an extinction of 1.050 for an 0.1 percent at 280 nm. CVF is relatively stable to heat and to alkali and acid. its specific activities as anticomplement and in hemolysis were 78.62 units per mg and 2691.5 units per mg respectively. These two properties are susceptible to activation by metal ions in the order $Mn^{2+} > Zn^{2+} > Ca^{2+}$ and to inhibition in the order $Co^{2+} > Mg^{2+}$. About 5 mM of EDTA were able to block the complement activation by CVF.

Synthesis of Peptide T—A Comparison Study

40091008C Shanghai HUAXUE XUEBAO [ACTA CHIMICA SINICA] in Chinese Vol 48 No 11, Nov 90 pp 1108-1112

[English abstract of article by Wu Tongde [0702 0681 1795], Chu Jiyu [5969 1323 3842] of the East China University of Chemical Technology, Shanghai, and Liu Yinzeng [0491 1377 2582] of the Shanghai Institute of Organic Chemistry, Academia Sinica, Shanghai]

[Text] Peptide T is a potential AIDS-inhibition peptide, which contains many hydroxyl side chains. Here, the synthesis of Peptide T by both Fmoc- and Boc-strategy on solid phase were compared. Yields are comparable and purity is better in Fmoc- than Boc-procedure. By-products were obtained by these two methods. Peptide T containing a t-butyl group was found in Fmoc-procedure and a benzyl group in Boc-method.

Cloning and Expression of Polyhedrin Gene From Insect Virus in E. coli Cell

40091009D Beijing WEISHENGWU XUEBAO [ACTA MICROBIOLOGICA SINICA] in Chinese Vol 31 No 1, Feb 91 pp 25-31

[English abstract of article by Qi Yipeng [7871 5030 7720], Huang Yongxiu [7806 3057 4423], et al., of the Department of Virology, Wuhan University, Wuhan; project supported by the National Science Foundation and the Foundation of National Education Commission]

[Text] The BamHI-H fragment containing polyhedrin gene (ocu) of Buzura suppressuria nuclear polyhedrosis virus (BsNPV) was inserted into BamHI site in plasmid pDR540 and two Ap^r positive recombinants were obtained. Total proteins produced by clones are more 1.1-2.4 folds than that by parent strain carried plasmid pDR540 in the medium. Expression of ocu protein was 0.8 mg/ml and 0.47 mg/ml. The expression protein was isolated and purified by PAG electrophoresis and gel chromatograph. The molecular weight is 32.1×10^3 dalton.

Cloning and Expression of Streptomyces lividans Promoters

40091009E Beijing YICHUAN XUEBAO [ACTA GENETICA SINICA] in Chinese Vol 18 No 1, Feb 91 pp 82-89

[English abstract of article by Huan Liandong [6703 6647 2767], Dong Kening [5516 0668 1337], et al., of the Institute of Microbiology, Academia Sinica, Beijing 100080; project supported by the National Natural Science Foundation of China]

[Text] BamHI restriction fragments from Streptomyces lividans TK24 chromosome DNA have been cloned into BamHI site of promoter probe plasmid pIJ486. Transformants were selected on the medium containing 5 μg/ml of neomycin. Four recombinant plasmids pMG1 (10.6 kb), pMG40 (7.6 kb), pMG50 (10.8 kb) and pMG88 (7.92 kb), were found and designated respectively. The inserted fragments in pMG40 and pMG50 were reduced to 0.78 kb and 2.2 kb by BglII digestion and rejoining. The different levels of neomycin and kanamycin resistance of these recombinant plasmids were determined. The results revealed that pMG50-25 showed a high level of neomycin resistance (90 μg/ml) and kanamycin resistance (500 μg/ml).

Molecular Cloning of Lipopolysaccharide Genes of the Vibrio Cholerae in E. coli HB101

40091009C Beijing WEISHENGWU XUEBAO [ACTA MICROBIOLOGICA SINICA] in Chinese Vol 31 No 1, Feb 91 pp 19-24

[English abstract of article by Shao Huang [6730 3552] and Ma Qingjun [7456 3237 6874] of the Institute of Biotechnology, Academy of Military Medical Sciences, Beijing]

[Text] A genomic library of the V. cholerae 178 (Eltor biotype, Ogawa serotype) was constructed by using cosmid pHC79 as a cloning vector. We screened the library with immune agglutination test and colonies solid phase ELISA. Thirteen positive recombinants which could express the O antigen of the V. cholerae lipopolysaccharide (LPS) were acquired. The LPS was then extracted from a positive recombinant PMM-VO38 by using hot phenol-water method. It was found that purified LPS specifically reacted to antisomatic serum against the V. cholerae. The restriction endonucleases analysis showed that the molecular weight of the recombination cosmid PMM-VO38 was about 46 kb.

Nitrogen-Fixation Research Project Bears Fruit

91P60167B Beijing RENMIN RIBAO in Chinese 27 Feb 91 p 3

[Article by Zhang Xuequan [1728 1331 0356]: "Nucleoprotein-Complex Found to Control Nodule-Formation Genes in Plants"]

[Abstract] Scientists Lu Jiaxi and Hong Guofan have discovered a nucleoprotein-complex substance with multiple binding sites that actually controls nodule-formation gene activity. It is known that the formation of root nodules depends on more than 10 genes in nitrogen-fixation bacteria, but the substance controlling gene activity has not yet been identified. Hong Guofan of the CAS Shanghai Institute of Biochemistry, who has been studying nitrogen fixation from the molecular genetics standpoint, has discovered that the trigger mechanism of the activities of 10 nodule-formation genes is controlled by one of those 10 nodule-formation genes. This trigger gene serves as a switch that can be turned 'on' and 'off' by a segment of nucleoprotein complex. The switch is turned on as soon as the nucleoprotein-complex segment binds to the trigger gene, which in turn activates the rest of the nodule-formation genes in nodule-formation bacteria and starts the root-nodule formation process. The discovery will help scientists understand the fine structure of nodule-formation genes and nodule-formation control mechanism, so that engineered artificial nodule-formation genes can be produced and genetically transferred to such crops as rice, wheat, and corn. Back in the 1970s, the former deputy director of the Department of Biology, Guo Xingxian, proposed the study of 'Chemical Simulation for Biological Nitrogen Fixation', which led to research work, the 'Structural Model of Molybdenum-Ferri-Sulfur Atomic Cluster of Nitrogen-Fixation Enzyme Activation Center'. In the Seventh 5-Year Plan, Lu Jiaxi synthesized a series of model cluster complexes containing transition elements.

Four Convex C120 Minisupercomputers Receive U.S. Commerce Department License for Export to China

91P60170 Beijing JISUANJI SHIJIE [CHINA COMPUTERWORLD] in Chinese No 12, 27 Mar 91 p 1

[Text] Four Convex C120 minisupercomputers for export to China have received an export license from the U.S. Commerce Department. These vector computers are intended for purposes such as seisomological petroleum prospecting, simulation of oil reserves, weather forecasting, and central weather research. Principal specifications of these computers are as follows: the combined vector/scalar CPU has a 64-bit word length, vector speed is 32 MFLOPS, internal memory is 128-256 MBytes, disk capacity is 4-10 Gbytes, number of tape drives is 2-4, number of terminals is 16-48, networks allowed are Ethernet and DECnet, and graphics workstations are included. The four computers are scheduled to arrive in China one after another between the end of March and the middle part of April.

On Implementing Chinese-Style CIM (Part II)

91FE0385A Beijing JICHUANG [MACHINE TOOLS] in Chinese No 1, Jan 91 pp 7-10

[Article by Li Kaifo [2621 7020 0154] of the Beijing Machine Tool Institute; for Part I, see JPRS-CST-91-004, 5 Feb 91, p 18]

[Text] **II. The Basic Concepts of a Chinese-Style CIMS**

CIMS must be designed based on the external environment and internal conditions of the industry, hence, there cannot be a unified Chinese-style CIMS. In this article we shall only explore the principle of a Chinese-style CIMS.

1. A Top-Down Overall Planning and a Bottom-Up Phased Implementation

The development of CIMS requires a long period of time, a large sum of investment, and a broad scope of involvement. It is therefore necessary to have an overall spatial and temporal planning beforehand. The top-down planning can only be an open model or skeleton. If the planning is too inflexible, there will be difficulties in making timely modifications, which can lead to technological and economic losses. A pure bottom-up phased implementation scheme, although possessing the advantage of small initial investment, fast effect, and flexibility, usually starts from a local consideration and lacks a systematic consideration. As the number of projects increases, more and more small machines will be bought and it is difficult to form a system in which the data can be shared. The bottom-up approach is poor in overall efficiency and may even cause difficulties in further integration and development.

Foreign experience shows that the two methods should be combined and the enterprise should gradually evolve toward CIMS under an overall guiding plan. With a weak foundation, China should especially pay attention to the three major elements of technology discussed in Part I of this paper. Without reliable components there will not be an integration. Therefore, the industrial application of CIM in China should follow the procedure of "foundation first, upper level next; components first, system next; local integration first, global integration next" under a general guiding plan. In the process, experience and talents will be gradually cultivated. The technology elements may be developed either in parallel or in series, depending on the condition of the enterprise. A safer approach is to develop more mature and urgently needed technologies so that results of one phase may be obtained and used as soon as possible.

It should be made clear that the subjects for CIMS are market products and not parts. Therefore, CIMS should cover the three major functions of design, manufacture, and management and involve everything for a product from market survey, purchase contract, and product sales. The flexible automation of the base level production should be based on the specialization of the technology and the components and the scope should not be too large in the beginning. There should be a clearly defined goal for CIMS and it should be consistent with the future development direction of the enterprise. The goal should be higher than the present production and management goals, but it should not be too idealized. It should be able to break through the bottleneck and capable of solving future problems.

The key to CIMS is integration and the top-down planning is to lay out a picture of an integrated enterprise in space and in time. The IDEF (for ICAM Definition Method) put forth by the U.S. Air Force, and the CIM-OSA (for open system architecture) put forth by ESPRIT in Western Europe were system analysis models. Both models were based on the requirements of production and operation and a functioning model was first built to reflect the mode of operation and basic activity of the enterprise. The information needs of an enterprise were analyzed and an information model was then built based on specific information relationships of the system and on the structure of the data bases. CIM-OSA may further generate resource models and organizational models.

2. Priority Should Be Given to Information Integration and Higher Open Structure so That MRP-II May Play a Key Role

As described above, a CIM system, via data sharing and data exchange, brings together the design (technology), manufacture and management, as shown in Figure 2. CIM will help China overcome the "slow, repetitious, and chaotic" problems in its industry. (Here "slow" refers to the slow pace in pricing, design, production preparation, information feedback, and delivery; "repetitious" refers to the chaos caused by extensive repetitions in copying, accounting, design and plan formulation.) In a Chinese-style CIMS, the automation of information should be placed at the top of the list in order to solve the problems of the timeliness, sharing, accuracy, and uniqueness of information. While improving computer assisted (CA) systems of engineering and management information, the machining of key components in the basic production process should also adopt CNC machines capable of achieving information flow automation.

Experience has shown that small and medium batches of advanced mechanical products cannot maintain their quality and delivery cycle without numerically controlled machines; without such machines the enterprise will also be lacking the ability to adjust to market changes and to renew its product lines. In China, however, due to the lack of capital, fully automated plants should not be attempted for some time yet and many of the machining and assembly operations still need to be done manually. The Chinese-style CIMS must therefore be highly open, it should not only integrate existing systems of automation or semi-automation, but also

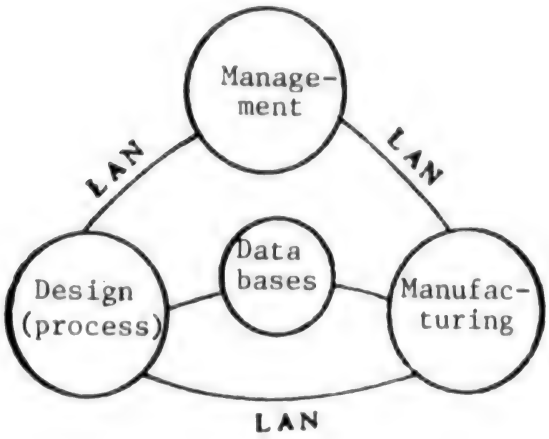

Figure 2. Conceptual Diagram of CIM

integrate future and more advanced subsystems of automation and explore ways to improve and integrate current manual subsystems in China.

At the Zhengzhou Textile Machinery Plant, after using NC machines and FMS machining for about 10 percent of their products, authorities plan to build a simple flexible machine shop to solve some of the problems in the machining of small and medium parts. The shop layout calls for the establishment of a number of machining units with both conventional lathe and NC machines based on the principle of three-dimensional warehouse and group technology (GT). Each of these units is equipped with a terminal and material in-out ports connected to transport carts. The primary function of the three-dimensional warehouse is to supply and deliver; storage is only secondary. The shop will have a management computer that is directly connected to the trunk communications network of the plant. The shop management computer takes assignments from MRP-II and, together with CAPP, arranges a two-day operation schedule. The computer is also linked to the material-flow computer and the terminals of the various machining units. This represents an attempt to improve the manual subsystems and integrate them into the CIMS of a plant using a combination of GT, MRP-II and CAPP technologies.

In a production system, human beings are the most active factor and also the most uncertain. Humans are creative and flexible, and are less likely to make mistakes due to other interference. Undeniably, the integration of the non-automatic production systems at the Zhengzhou Textile Machinery Plant will require human intervention and this intervention will affect the timing of the signals and may lead to errors in the transmission and acquisition of signals. This approach appears to be a loose form of integration and is usually a transition toward more highly integrated systems. Therefore, in planning this type of system, room should be left for future expansion and for improvement in the degree of integration. This kind of "quasi-integration" production system will have a practical significance in China for some time to come. We should therefore develop good man-machine interfaces and effective error-prevention measures. Of course, the Zhengzhou Textile Machinery Plant has only begun to explore this area and the system will be improved and perfected in the practice. The intention of the author is only to express some views on the more controversial issues and to stimulate discussion.

Because the degree of automation in China's low-level production processes is rather limited, it is particularly important for MRP-II to play a major role in the progress and capability planning, monitor and control of the entire production process (including automated and manual steps) in a Chinese-style CIMS. CAQ, often mistaken to be a quality control of the low-level production process, should actually be present throughout all activities and is the total of all quality planning, management and control. Based on these considerations, the author devised a Chinese-style CIMS for the present situation. This CIMS is shown schematically in Figure 3.

3. Organize Production Based on the Principle of GT and Specialization; Stress the Role of Human and Software Technology in Low-Level Production

Since the soft automation technology of thermal processes (casting, forging, etc.) is not yet mature and in view of the need to follow the principle of specialization, the scope of China's CIMS should be concentrated in machining and assembly. At this time the emphasis of soft automation should be placed on the machining of key components, but the problem of poor quality of blanks must also be solved as well.

The conventional method of organizing production according to the product can still work for large-batch production of relatively fixed products. When machine groups are used for the production of small or medium batches of a variety of products, however, the manufacture process becomes difficult to manage and the length of production preparation and machine adjustment periods will be lengthened. Materials are often found to be missing during the setup and the enterprise's ability to compete will be compromised.

When MRP-II is combined with GT, a manufacturing center is set up in a timely manner according to the MRP-II management plan, and the production preparation and manufacturing organization are conducted according to the "component group." In this approach, there is not only the benefit of an expanded batch volume but also a more stable production system and the ability to apply different manufacturing means to different components. The Jinan First Machine Tool Plant and the Shenyang Blower Plant have already made considerable progress in this area.

Different types of parts will be made using different manufacturing organizational methods. For general parts, it is best to use a lateral distribution of plants, leaving the lead plant to make only the key components.

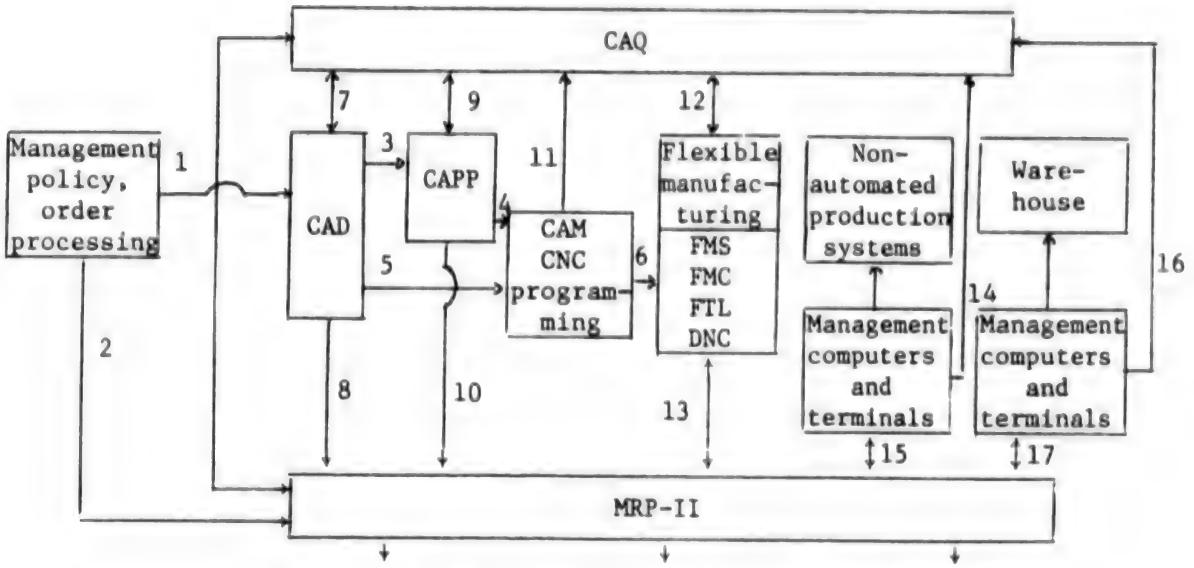

Figure 3. The Author's Concept of a Present-Stage CIM

1—Product design requirements; 2—Ordering and production scheduling; 3—Geometric data for technology planning; 4—Technology and tool data; 5—Geometric data for writing NC programs; 6—NC data; 7—Performance targets and geometric data (upward); 8—Part-list (BOM) data; 9—Work-plan data, to form quality-control plan and inspection codes (upward) and feedback and control data (downward); 10—Work-plan data included into MRP-II for general management; 11—Numerical-control programs of CNC measurement devices; 12—Measurement data in the process (upward) and control data (downward); 13—Production task assignment and operation-plan data (upward) and production-data acquisition and interference feedback (downward); 14—Quality testing data (upward) and testing plan and codes (downward); 15—Production task assignment and operation plan data (upward), and production data acquisition (downward); 16—Quality data acquisition for external items (upward), and receiving inspection plan for purchased external items (downward); 17—Storage and transfer plan (upward), and acquisition of storage status data (downward).

Of course general parts may also be made using a combination of MRP-II, GT and CAPP, like those in the Zhengzhou Textile Machinery Plant.

There have been efforts overseas for highly flexible FMS but the economic benefits were less than satisfactory. In China, the stress on FMS is not on the high flexibility but on the ability to adapt to market changes and product renewal. The overall principle for the foundation-level CIM is to allow man-machine interaction and to suitably decrease the degree of automated material flow while ensuring the automated flow of information. Therefore, there should not only be highly automated FMS or FMS at the foundation level in China's CIM system, but also quasi-FMS. DNC and machining units where the material loading-unloading and transport are not automated. Even in FMS, the transport of cutting tools and the loading of materials on the trailing pallet may be done manually instead of with robots.

In China, because of the low level of associated technology, attention must be given to the reliability and stability of NC machines and industrial robots. The role of software should also be stressed because the manufacturing standards may be improved and greater benefits may be obtained through the use of software (such as mold simulation, dynamic adjustment and management, on-line quality assurance, and intelligent fault diagnosis). Generally speaking, the entire CIMS should reflect the concept of "hardware as the foundation and software as the key."

Assembly is an important step in manufacturing and sufficient attention must be given to this step. Because of capital and technology reasons, only a small fraction of manufacturing in China is partially automated. Most production (e.g., aircraft and machines) still relies on the ability of the workers and could be improved by strengthening MRP-II management, modifying assembly equipment, and the storage and transport of parts. The proportion of humans, hardware, and software in China's fundamental CIM system is shown in Figure 4.

4. Strengthen the Basics, Carefully Select the System, and Improve the Human Aspects of the Effort

Building a CIMS is a long-term effort of considerable complexity. The enterprise leaders should be prepared to make a long-term investment and overcome difficulties

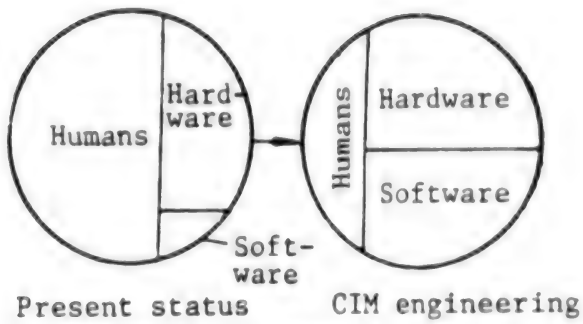

Figure 4. Proportion of Humans, Software, and Hardware in Chinese-Style CIMS

that arise on the way. In order to reduce the difficulties in integration, the following problems deserve special attention:

(1) Simplification, standardization, and serialization are prerequisites for integration.

To put it simply, the idea is to "slim down" and the effort should take place in all the business activities including manufacturing, processing, production organization and operations. The goal of simplification is to reduce the number of signal sources and to compress the amount of signals. We should therefore first simplify the source for production signals—the products themselves. While we simplify the product structure, we must also pay attention to the simplification and unification of part shapes and dimensions. In addition to signal simplification, product simplification, and product unification, the product structure should also be modularized. Other contents of the simplification effort include the specialization of production, typification of manufacture process, and the condensation of the organization.

Foreign experience shows that without standardization there will not be any CIMS. Not only the data format and communications interfaces must be standardized, the dimensions of the trailing pallet, the height of the workbench on a machine, the spare parts, process planning, operation planning, design and process documentation format, and even the standardization of certificates and tags all have a direct effect on the integration.

In the manufacture of small and medium-batch products, GT is not only the basic principle for organizing the production but also the "unifying" technology for design, process, manufacture, and management. Part-number coding based on GT reflects this "unifying" effect. An important basic work is to replace the traditional serial numbers with CIMS-compatible codes (i.e., product model number + component number + part number).

In order to make better use of the data and the principle of production by groups, it is imperative that some adjustments be made to the organizational structure and manufacturing operations of the enterprises. In making these adjustments, however, attention should be given to both continuity and improvement so that people can accept these gradual changes.

(2) Carefully select the computer systems and supporting accessories.

With regard to the selection of computers, based on the author's experience visiting some enterprises, the great majority will still use the layered structure. Figure 5 shows the basic plan of the layered computer structure.

In Figure 5, the small or medium computers serve as the central processing units. There are usually two units, one unit responsible for processing technical information (mainly CAD/CAM at this time) and the other responsible for processing business information (MRP-II). The first task requires a high speed, a large internal memory and a strong ability to process graphics. The second task mainly requires large (external) storage. Of course there are also microcomputers being used as CPUs. For CAD/CAM purposes, workstations are more flexible and are often connected to the technical information CPU. For FMS the computer must be reliable and interference-proof in the production environment; industrial microcomputers should be used whenever possible.

The following are the main considerations for computer selection: 1) Compatibility of hardware and software and concentration of suppliers. Buying one from each country is not recommended. 2) Continuity, especially the continuity of operating systems and data bases already exist in an enterprise. 3) Give Chinese-made mainstream machines the priority. 4) High performance and sufficient capacity for future demands. 5) Availability of open software and ability to handle Chinese characters. 6) High reliability of hardware and good after-sales service.

The structure of the data bases depends on the overall design, but the structure will definitely be of the distributed type. A number of enterprises prefer the connected data base and management system. It appears that CAD/CAM may take advantage of the connected data

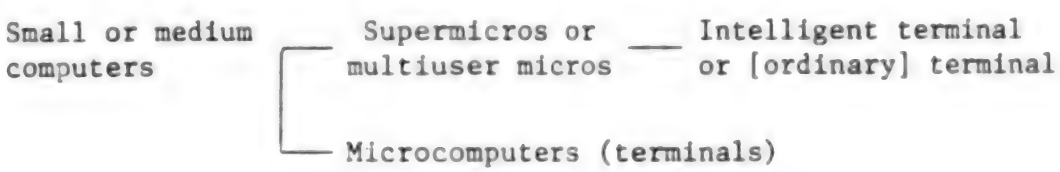

Figure 5. Layers of Computers

bases and deliver BOM data to MRP-II. The exchange of CAD graphics data is presently done through the basic graphics-exchange system (IGES), but it will eventually be implemented using the product model data-exchange procedure (STEP) being formulated by ISO.

Local networks connecting the entire plant are essential support systems of CIMS. In order to solve the high-speed communications problems between odd model computers in the industry, the main network of China's CIM will use the manufacturing automation protocol (MAP). Today's MAP is version 3.0. Upper-level CIM communications between CAD/CAM and MIS (MRP-II), because of the shorter distances and the lesser need for real-time operations, can be satisfied with an Ethernet that uses the CSMA/CD (carrier sense multiple access with collision detection) mode of communications. Similar nets include specific ones like DEC-net. Upper-level subnets should best be from existing resources of the business and not necessary TOP (Technical and Office Protocol) nets. Within the FMS, there is obviously the need for real-time control. The RS232C interface used today has a maximum speed of 19,200 bps. In the past the communications mode was based on star-shaped point-to-point communications, but that technique's low speed cannot satisfy the CIMS requirements. In the long term we should still use MAP nets, especially the simpler and cheaper mini-MAP subnets. Due to the high costs of MAP interfaces and the incomplete standardization, not too many FMS are using MAP nets.

(3) The human factor

It is people who develop CIMS; it is also people who resist CIMS and people who perfect the CIM technology. The success or failure of CIMS depends on people. Experience shows that CIM requires an enterprise to change some of its old habits, but habits are hard to break, not to mention man's hesitation to adopt anything new. It is extremely important that we unify the ideological understanding, cultivate a healthy attitude toward CIM, and improve the technical education and business standards.

To achieve this, the following must be done: 1) The leadership must unify the ideological understanding, the middle-level cadres must do a good job, and the entire plant must be mobilized in its thought process. 2) Establish a CIM general group consisting of the leaders of the enterprise and principal staff, and a number of implementation groups under it. The CIM general group is best headed by the plant director. 3) There should be all-staff training; the emphasis should be on the training of the plant-level and middle-level leaders and technical and management personnel, and different courses should be provided to different people.

III. Concluding Remarks

To develop CIM in China is not just to follow a trend, it is also to satisfy the practical needs to convert China's machine manufacturing enterprises from extensive management to intensive management. The conversion, however, must suit the particular situation in China and adopt appropriate development strategies and implementation methods. As long as the strategy is correct and the implementation is proper, CIM will definitely contribute to the revival of China's machine industry.

The author has participated in the on-site investigation of priority CIM engineering projects. The opinions expressed in this article regarding development strategy naturally contain the author's own interpretation of the instructions of the State Science Committee and the experts' council. Some of the views expressed in the group discussion of the investigation group were also included. Some of the views in the second part of this article are purely exploratory, and the materials are mostly from the on-site investigations. This article is only one man's opinion and may contain unavoidable errors; the author welcomes critique and corrections.

New Technique for Laser U-Isotope Separation Passes Feasibility Appraisal

91P60168B Beijing KEJI RIBAO [SCIENCE AND TECHNOLOGY DAILY] in Chinese 2 Mar 91 p 1

[Artile by Fu Ke [1788 4430]: "New Advances Realized in Laser Uranium-Isotope Separation Research"]

[Summary] The "laser selectivity activation chemical reaction technique for uranium-isotope separation" (or CRISLA), a State Education Commission priority S&T project jointly undertaken by Fudan University, Sichuan University, and Dalian University of Technology, passed expert feasibility appraisal a few days ago at Fudan University in Shanghai. The experts noted that this project has tracked the newest developments worldwide in laser isotope separation (LIS) of uranium.

The CRISLA technique, one of the newest methods recently developed worldwide for LIS of uranium, is a key step in the production of enriched nuclear fuel, and has advantages—such as lower cost and lower energy consumption—over the older techniques of gaseous diffusion and gas centrifuge. In view of the fact that industrial-scale development of LIS techniques would generate enormous economic benefits, several nations have been pushing forward with LIS research in recent years, and China too has devoted much attention to this topic, as evidenced by the recent advances at the aforementioned three institutions.

Krypton-Fluoride Excimer Laser Debuts

91P60168C Beijing ZHONGGUO KEXUE BAO [CHINESE SCIENCE NEWS] in Chinese 22 Mar 91 p 2

[Article by Peng Dejian [1756 1795 1696]: "Krypton-Fluoride Excimer Laser Unveiled"]

[Summary] Hefei—CAS's Anhui Institute of Optics and Fine Mechanics has recently developed a practical long-pulse, low-divergence-angle Kr-F excimer laser. This is the first practical electric-discharge-pumped unstable-cavity excimer laser developed domestically, and leads Chinese-developed excimer lasers in terms of pulse energy, beam divergence, pulse width, delay jitter, and pulse energy stability. According to the user's needs, this device can provide a laser output at a 248-nanometer wavelength (KrF) or—via substitution of the gas—at a 308-nanometer wavelength (XeCl). The new excimer laser has applications in laser chemistry, laser isotope separation, laser spectrometry, surface physics, laser medicine, and laser remote sensing.

Experimental Coherent CW-CO_2 Laser Imaging System

91FE0323B Shanghai GUANGXUE XUEBAO [ACTA OPTICA SINICA] in Chinese Vol 10 No 12, Dec 90 pp 1097-1101 [MS received 15 May 90, revised 20 Jun 90]

[Article by Fan Liming [2868 4539 2494], Nan Jingda [0589 0079 6671], Jia Liejuan [6328 0441 1227], and Pi Mingjia [4122 0682 0857] of the Department of Applied Physics, Harbin Polytechnic University: "Experimental Coherent Continuous-Wave CO_2 Laser Imaging System"]

[Text] **Abstract**

A prototype coherent continuous-wave (CW) CO_2 laser imaging system is described. Experimental coherent imaging results involving one and two point targets are reported. Certain factors affecting the imaging quality are also discussed. With slight modification, this system can be used in velocity and 3-D range imaging.

I. Introduction

In 1966 Teich et al. studied the heterodyne effect at 10.6 μm.[1] Because coherent laser imaging has a great deal of potential in military applications, atmospheric and environmental monitoring and air traffic control, it has been studied in detail. A number of prototype coherent laser imaging systems have been developed.[2,3]

A laser radar is a product combining laser technology with radar technology. Because the laser wavelength is several magnitudes higher than that of microwave, laser radar is far more superior to microwave radar in terms of accuracy, resolution and interference resistance. A coherent laser imaging radar is an active detection system. Compared to a passive detection system such as a thermal imaging system, coherent laser imaging can simultaneously provide velocity, range (3-D range) and profile while thermal imaging can only provide a thermal radiation temperature difference pattern. Laser imaging radar can be divided into direct reception and coherent reception. It has been proven in theory and practice that coherent laser reception technique offers higher sensitivity and can deliver more information about the target.[4]

Figure 1 shows the block diagram for a coherent laser radar. The transmitting laser is emitted from an optical antenna through the atmosphere to interact with the target. Characteristics of the target (such as velocity, surface reflectance, etc.) carried by scattered light are processed by the reception system to obtain static and dynamic information of the target such as velocity, range and location.

A prototype coherent CW-CO_2 laser imaging radar system is described in this paper. Certain factors affecting the imaging quality are discussed and some experimental results are reported.

II. Experimental System

Figure 2 shows the schematic diagram of the experimental coherent CW-CO_2 laser imaging system. The local-oscillator light and the transmitted light are the 10P(20) line of the CO_2 laser at 1 W and 2 W, respectively. The frequency difference of the two lasers ω_{if} was fixed at 30 MHz by adjusting the PZT [piezoelectric transducer] resonant cavity. Both lasers were in the

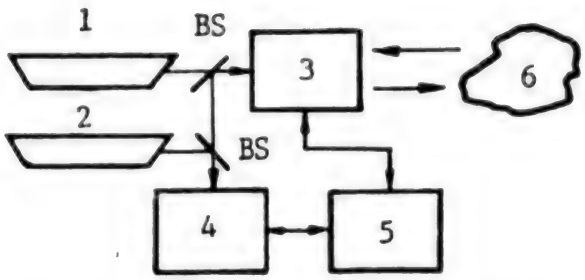

Figure 1. Block Diagram of Coherent Laser Radar

Key: 1—transmitting laser; 2—local oscillator; 3—transmitting-receiving optical antenna; 4—receiving system; 5—processing and controlling system; BS—beam splitter

TEM_{00} output mode. A passive frequency stabilization technique was used to stabilize the laser output. Frequency mixing took place on the single-element HgCdTe detector. The frequency-response range of the detector is 20 MHz to 200 MHz. The output signal from the HgCdTe detector may be directly input into a computer to be recorded, processed and displayed after amplification and detection, or may be plotted out by an X-Y recorder for further analysis.

The beam expansion telescope used is an improved reflective Cassegrain telescope[5] (shown in Figure 2 as the dotted block). The beam expansion ratio is 10:1. The light output is approximately 20 mm in diameter and the beam expansion mirror is gold coated. The dynamic field of view (FOV) of the telescope is too small to satisfy the need in real life. A laser scanning system was employed to expand the dynamic FOV in order to scan, sample and capture target patterns in space. The scanner has a mechanical scanning mirror whose dynamic FOV is 360° x +/-7.5°.

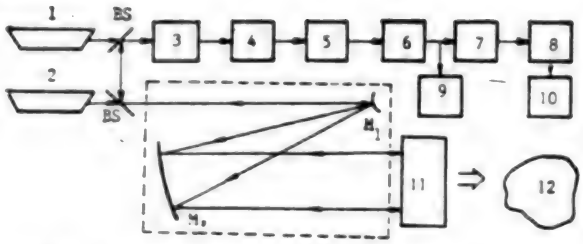

Figure 2. Schematic Diagram of the Experimental Arrangement

Key: 1, 2—CO_2 laser [10.6 μm, 10P(20)]; 3—HgCdTe detector; 4—pre-amplifier; 5—liner amplifier; 6—diode detector; 7—A/D face; 8—STM personal computer; 9—X-Y recorder; 10—image monitor; 11—laser scanning system; 12—target; M_1, M_2—reflector; BS—beam splitter

III. Experimental Results and Analysis

Figure 3 shows system calibration results with no target in sight. Different electrical signals will be produced with respect to a different relative position between the laser scanner and the optical axis of the optical system. When the scanning mirror is on the optical axis, as shown in Figure 3(a), the detection system has four pulses as shown in Figure 3(b). These four pulses correspond to reflected (scattered) signals from four sides of the scanning mirror, respectively. When the scanning mirror is off the optical axis, as shown in Figure 3(c), two scattered pulses are eliminated as shown in Figure 3(d). This indicates that when the scanning mirror is on the optical axis, there are two extra noise signals. This is extremely unfavorable for target identification and data processing. Therefore, the scanning mirror was placed off the optical axis as shown in Figure 3(c). Pulse A can be used as a reference for the position of the scanning mirror. Pulse B can be eliminated by treating the back of the mirror. Or, a double-faced mirror may be used to consolidate A and B.

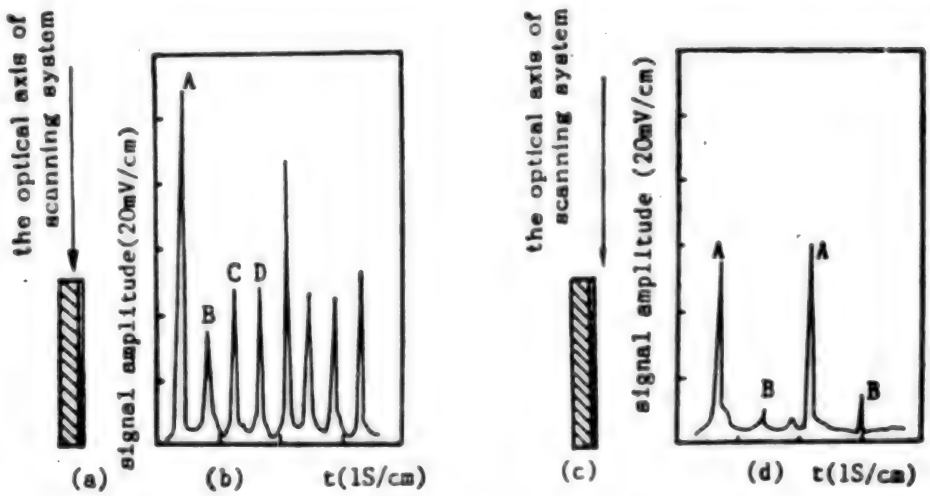

Figure 3. Output of HgCdTe Detector With Scanning System Adjustment (no target)

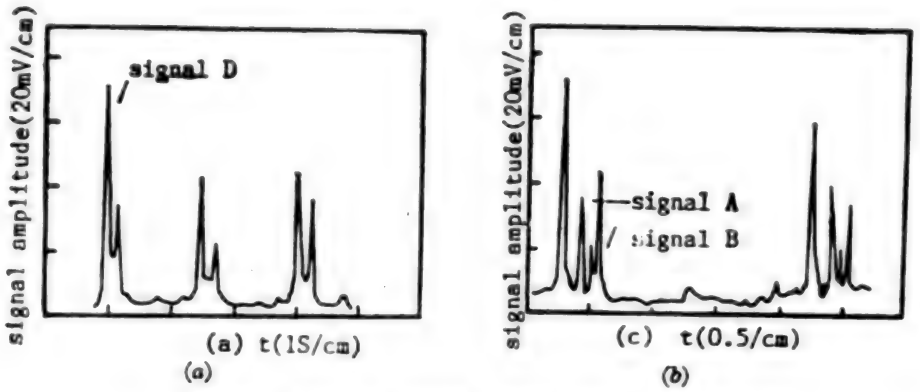

Figure 4. Electrical Signals Recorded by X-Y Recorder

Within a +/-10° x +/-7.5° FOV, imaging of a single point target and a two-point target was studied. The results are shown in Figure 4. Figures 4(a) and (b) are X-Y recorder plots of the electrical signals (horizontal scanning, vertically stationary). Figures 4(a') and (b') [photos not reproduced] are the target reflection (scattering) intensity patterns processed by the computer. The targets are a 100-mm-diameter plane mirror and spherical mirror located 2 meters away from the center of the scanning mirror. The picture shows 16 colors (STM microcomputer). The bright spot at the upper left corner shows the size of the image element. The 16 colors represent relative intensities of 15, 14, ..., 1, 0, from left to right in decreasing order.

In Figure 4(a), immediately next to the reference signal D is the plane-mirror echo signal. Figure 4(a') shows the corresponding target picture. In Figure 4(b), A and B are the echoes from the plane mirror and spherical mirror, respectively. The small pulse in between is the echo from a small mirror at a distance. The angle is approximately 5°.

In Figures 4(a) and (b), the signals recorded are much wider than the pulse widths of the electrical signals. This is because it is impossible to match the recorder with the scan rate. In Figure 4(b), B is wider than A. Signal B corresponds to a concave mirror which has a larger FOV compared to a plane mirror. From Figures 4(a) and (b) it was found that the signal amplitude varies randomly with time. Statistical analysis of the targets shows that it follows the Ricean distribution for mirror type of targets. In addition, instability of the laser output also causes signal variation. In order to eliminate random effects, statistical treatment has been incorporated in signal processing.

IV. Conclusions

There is excellent agreement between experimental results and design. Due to a scan-rate constraint, the imaging speed is limited to 0.5 frame/min. By increasing the scan rate further, it can reach 10 frames/min. The authors are developing a high-accuracy, high-speed laser scanner to increase imaging speed and spatial resolution. Profiles of one-point and two-point targets were obtained after data processing. With minor modification, the system can be used in velocity and 3-D range imaging.

The authors wish to express their gratitude to Professor Dai Yongjiang [2071 3057 3068] and Senior Engineer Li Yimei [2621 5030 5019] for their assistance.

References

1. M. C. Teich, et al., APPL. PHYS. LETT., Vol 9, No 10, Nov 66, pp 357-360.

2. A. B. Welch, B. Burzlaff, et al., PROC. SPIE, Vol 300, 1981, pp 153-162.

3. E. R. Washwell, et al., PROC. SPIE, Vol 415, p 39.

4. P. A. Forrester and K. F. Hulme, OPT. & QUANTUM ELECTRON., Vol 13, No 4, Jul 81, pp 259-293.

5. K. Gullberg and A. Widen, AD-a146670.

Free Electron Laser With Grazing Incidence Ring Resonator

91FE0323A Shanghai GUANGXUE XUEBAO [ACTA OPTICA SINICA] in Chinese Vol 10 No 12, Dec 90 pp 1075-1079 [MS received 17 Apr 90, revised 30 May 90]

[Article by Wang Mingchang [3769 2494 1603], Yuan Youlong [5913 1635 7893], Feng Bibo [1409 4310 3134], Zhou Huifen [0719 1979 5358], Feng Chengshi [7458 6134 1102], and Wang Zhijiang [3769 0037 3068] of the Shanghai Institute of Optics and Fine Mechanics, Chinese Academy of Sciences: "Free Electron Laser With Grazing Incidence Ring Resonator"]

[Text] **Abstract**

A novel free electron laser (FEL) resonance cavity structure is investigated. Using a combination of hyperboloid-paraboloid mirrors, the diameter of the beam inside the cavity can be expanded by approximately six times. Thus, the resistance of the reflective coating against laser

damage is improved. The effects of parameters such as beam expansion factor, aspherical parameter, resonance cavity length and grazing spot size on the aberration of the optical system are also discussed.

I. Introduction

An optical resonance cavity is a key component of a laser oscillator. It affects the establishment, power build-up and saturation of the laser oscillation and the quality of the beam output. Different from a conventional laser, an FEL has a new set of design requirements for its optical resonance cavity. The electron beam is the medium to generate radiation. It requires total match in time and space between the electron beam and the light beam in the cavity. Furthermore, due to the fact that the oscillating magnetic field gap of the FEL is small (approximately 1 cm) and cavity length is long (1-3 m), usually a concentric, confocal structure[1] is used. As for the output coupling, it is total reflection on one end and partial transmission on the other. This arrangement will be difficult with a high-power FEL output, since one of the characteristics of an FEL is high power and high efficiency. The power density inside the cavity is very high (hundreds of MW/cm^2 to thousands of MW/cm^2).[2] Power damage to the reflective mirror in the resonance cavity is one of the pending FEL design problems to be resolved.

Using a concentric cavity structure, the size of the spot on the mirror can be increased. In a structure with a long oscillating magnetic field and small gap, the oscillating light suffers significant diffraction loss at the entrance and exit of the magnetic field. An earlier method is to lengthen the cavity to enlarge the spot on the mirror in order to lower the energy density. However, some new problems emerge after the cavity is lengthened. The device becomes cumbersome. A long cavity makes the output power more sensitive to the tilt of the reflective mirror. More accurate adjustment of the mirror is required. More importantly, the pulse width of the radio-frequency (rf) FEL electron beam is generally around 10 μs, the time for one laser oscillation is 2 L/3, and in order to maintain sufficient number of oscillations, the cavity length L cannot be too long. In order to lower the power density taken by the mirror, Bhowmik proposed a grazing incidence ring resonator.[3] Without any doubt, this opened a new area in the study of resonators. Nevertheless, it is not easy to obtain high-quality laser characteristics and minimize aberration in such a complex optical system. Moreover, reference 3 did not quantitatively determine the effect of various structural parameters on aberration.

In the present work, a resonator with a beam expanding system consisting of hyperboloid-paraboloid mirror assembly is designed. It expands the diameter of the oscillating beam by a factor of six to improve the resistance of the mirror against laser damage. In this paper, based on geometric optics, the effects of various parameters such as beam expansion factor, aspherical parameter, cavity length and grazing incidence spot size on the aberration of the optical system are determined. The authors believe that this novel optical design can create a new avenue in the study of rf FEL resonators.

II. System Structure

Figure 1 shows the grazing incidence ring resonator cavity. This is a confocal, non-coaxial hyperboloid-paraboloid telescope system. The telescope incident cross section is the central optical waist w_0 of the wobbling magnetic field W. The light beam enters the hyperbolic mirror at a large grazing incidence angle and is then reflected onto the parabolic mirror. Afterward, it becomes a parallel beam. It returns back to the optical waist after going through another paraboloid-hyperboloid telescope system to complete one cycle in the cavity. AB and BC are the revolving axes of the hyperboloid and paraboloid, respectively. B is the common focus and A is the other focus of the hyperboloid.

Let us consider the meridian plane ($z = 0$), in which the revolving hyperboloid equation is

$$y^2 = 2Rx + (m-1)x^2. \qquad (1)$$

The revolving paraboloid equation is

$$y^2 = 4fx \qquad (2)$$

where R is the radius of curvature of the apex of the hyperboloid, m is a parameter of the hyperboloid; the

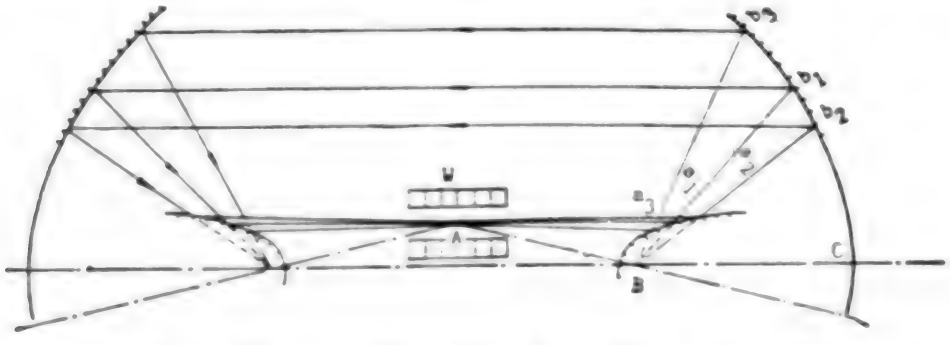

Figure 1. Schematic of FEL With Grazing Incidence Ring Cavity

angle between the hyperboloid and paraboloid on the meridian plane u_0 is determined by computation, and f is the focal length of the paraboloid.

The incident light intersects with the hyperboloid at a_1, a_2 and a_3 The subscripts, 1, 2 and 3 are used to represent the middle, upper and lower light beam on the meridian plane. The light intersects with the paraboloid at b_1, b_2 and b_3. Let us define $L_1 = Aa$ and $L_2 = aB$. The magnifying factor of the hyperboloid is $g = (L_1/L_2)$. Let u_0 be the angle between incident light ab and axis AB (x-axis) and u_i be the angle between reflected light ab and axis AB, θ_i is the angle of incidence on the hyperboloid, and dy is the width of the reflected light beam on the meridian plane.

The computation program was designed based on the light tracking method in geometric optics to study the relation between various parameters. The center incident light is parallel to the optical axis of the paraboloid. The origin is chosen at the apex of the paraboloid C, BC is the x axis and the y axis is as shown in Figure 1. In a Seidel imaging system, the laser waist is considered as a geometric point. In such a structure, A and B are points on the axes of two revolving aspherical planes. It is even more complicated for points off these axes.

Because the field angle of the spot with respect to the system is very small at the waist, the sinusoidal difference of off-the-axis points can be neglected. However, because the two revolving planes are used off-axis and are non-coaxial, the magnifying factor varies at different position at the pupil. This leads to emergent light deformation (pupil deformation).

After taking factors such as beam magnifying factor (i.e., aperture of parallel beam b) and pupil deformation (only considering asymmetry of upper and lower light beam with respect to the middle beam on the meridian plane) into account and considering the fact that grazing area on the hyperboloid cannot be too small, the program performs artificial "intervention" to control the magnifying factor of the hyperboloid g and focal length of the paraboloid f. An ideal profile was obtained. In addition, various aspherical parameters such as P, m and R and angle α were also determined.

The spot size from grazing incidence onto the hyperboloid is $(\cos\theta_i)^{-1}$ times larger than that of normal incidence. Assuming the incidence range is $80° < \theta_i < 87°$, then the spot on the mirror is increased by a factor of $5.8 < (\cos\theta_i)^{-1} < 19$. The energy density taken by the mirror is lowered by the square of this factor. Furthermore, the reflectance of most dielectric and metal films is close to 1 within this incidence angle range.

III. Design Results and Discussion

The optical computation program is to use the focal length of the paraboloid f as a variable to calculate the beam expansion factor η, optical cavity deformation Δy and radius of curvature at the apex of the hyperboloid R based on a set of given parameters such as cavity length L, short axis of the hyperboloid b and magnifying factor g.

By properly choosing g-f, it is possible to minimize the light deformation on the meridian plane (minimum asymmetry of upper and lower light with respect to the middle light beam). In the system, if two plane mirrors are introduced symmetrically on the right and left side, then the imaging of the parallel beam is at -1. Therefore, the system is at +1 at the waist. In this case, the pupil deformation effect is eliminated.[5]

The beam expansion factor η is defined as the ratio of parallel beam cross section to incident pupil cross section. A graph of the beam expansion factor η as a function of g and f is shown in Figure 2. Using f as a variable, η increases with increasing g. If g remains constant, η goes up as f increases.

The long half axis of the hyperboloid mirror is a and its short half axis is b. There is a relation $b^2 = c^2 - a^2$. The focal length of the hyperboloid is $f' = c-a$. The radius of curvature of its apex is $R = 2f'$. Based on the curves shown in Figures 2 and 4, b is chosen to be 250.0 mm.

In order to ensure grazing incidence, the value of b is extremely limited due to the size of the reflective mirror; b_{max} differs with different g. As shown in Figure 3, b_{max} does not decrease linearly with increasing g. Its range is between 200 and 1,000.

Define the pupil deformation parameter as Δy, which is the difference of upper and lower beam cross section. Figure 4 shows the Δy versus g curve at various f values. Pupil deformation increases monotonically with g and also increases significantly with f.

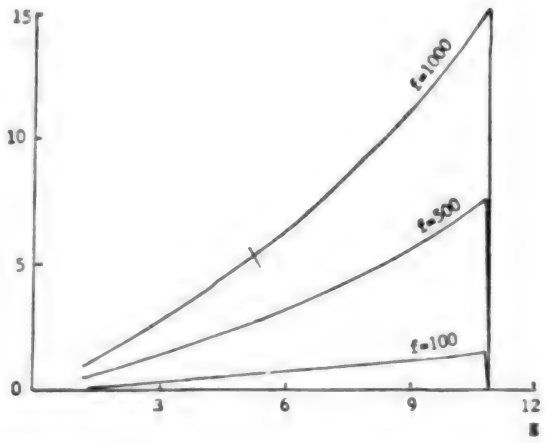

Figure 2. Dependence of the Beam Expansion η on the Magnification of Hyperboloid g. Focal length of the paraboloid f is a variable parameter.

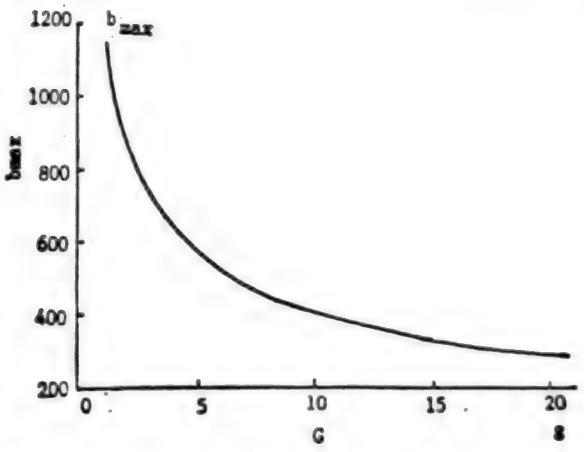

Figure 3. Maximum of Hyperboloid a_1 Short Axis b_{max} Versus g

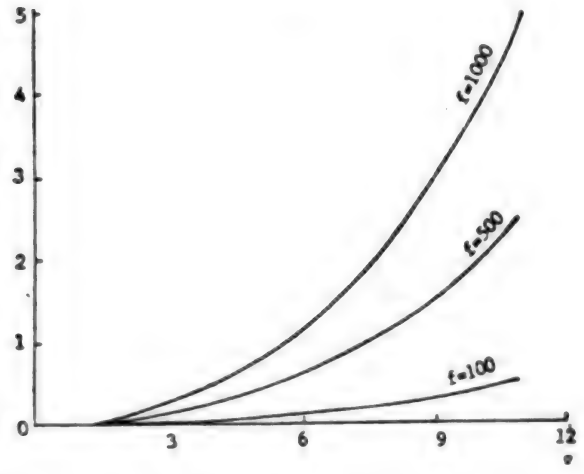

Figure 4. Pupil Deformation Δy Versus g, f is a Variable Parameter

The magnitude of Δy in essence has an impact on the deviation of the parallel beam away from the center axis. It is extremely unfavorable to place the output coupling mirror at the parallel beam. Therefore, Δy must be minimized.

Based on calculated results, a set of typical resonant cavity parameters are listed in Table 1. In addition, characteristics of the paraboloid and hyperboloid are also listed.

Table 1. Typical Parameters of a Cavity

System parameters	
Length of cavity	L = 2,500 mm
Cross section of I.P.	d = 8.7 mm
Cross section of E.P.	D = 49.5 mm
Expansion magnification	= 5.7
Pupil deformation	y = 0.7 mm
Wavelength	= 1.06 μm
Hyperboloid	
Incidence angle	= 83.8°
Large half axis	a = 312.5 mm
Short half axis	b = 100.0 mm
Radius of curvature	R = 32.0 mm
Charact. parameter	m = 1.1
Magnification	g = 2.0
Focal length	f = 3,500 mm

The typical resonator is a structurally sound resonator that can be fabricated. For example, the b of the hyperboloid can neither be too large nor too small. Because of aberration Δy, it is better for g to be around 2. From Figure 2, the beam expansion magnification η cannot be very large. Furthermore, the range of b_{max} can be estimated from Figure 3.

Optical computation shows that a confocal hyperboloid-paraboloid telescope structure offers the best optical imaging quality. Such a non-coaxial system makes the discussion of aberration more complicated. In this paper, it is limited to the meridian plane. Discussion involving a sagittal plane will be published in a separate paper.

References

1. Wang Mingchang, Wang Zhijiang, et al., ZHONGGUO JIGUANG [CHINESE JOURNAL OF LASERS], Vol 17, No 7, Jul 90, pp 40-44.

2. S. V. Benson, J. M. J. Madey, et al., NUCL. INSTRUM. METHODS PHYS. RES., 250A, 1986, pp 39-43.

3. A. Bhowmik, R. A. Cover, et al., IEEE J. QUANT. ELECTRON., Vol 24, No 5, May 1988, pp 802-811.

4. Wang Zhijiang, "Fundamental Theory in Optical Design," Science Publishing House, Beijing, 1985, p 296.

5. C. C. Shin, "FEL Resonator," Beijing Institute of Modern Physics Series, Vol 2, 1988, p 286.

Microwave Emission from a Virtual Cathode Source

91FE0193A Chengdu QIANG JIGUANG YU LIZI SHU [HIGH POWER LASER AND PARTICLE BEAMS] in Chinese Vol 2, No 3, Aug 90 pp 319-323

[Article by Wang Pingshan [3769 1627 1472], Hu Kesong [5170 0344 2646], Huang Sunren [7806 1327

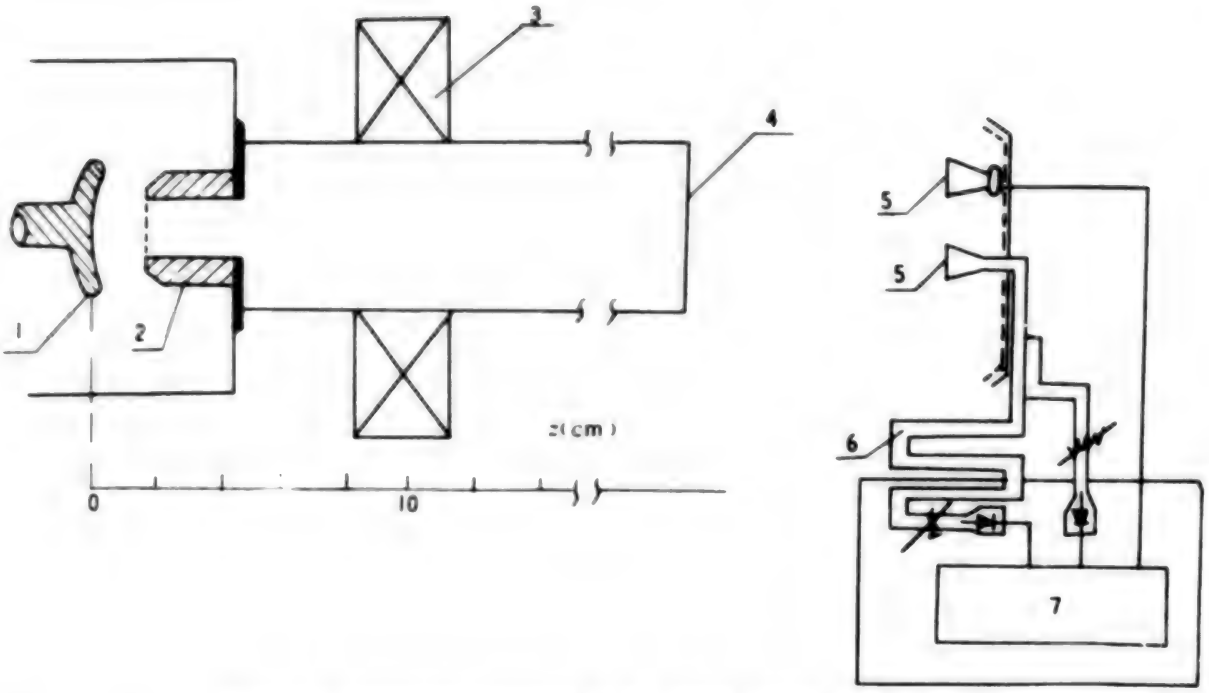

Figure 1. Experimental Apparatus for the Virtual Cathode Radiation Device

Key: 1. cathode, 2. anode, 3. short magnetic lens, 5. receiving horn, 6. dispersion line, 7. oscilloscope

0088], Chen Yutao [7115 5940 3447], Deng Zhaohui [6772 2600 6540], Fu Shuzhen [0102 3219 3791] and Xu Yong [1776 0516] of Southwest Institute of Applied Electronics: "Microwave Emission from a Virtual Cathode Source"; MS received 18 Sep 89, revised 1 Dec 89]

[Abstract] Due to advantages such as high power and high efficiency, a great deal of theoretical and experimental work has been done on the Vircator (Virtual Cathode Microwave Radiation Device). This paper describes a virtual cathode microwave radiation experiment performed on the EPA-74 pulse linear accelerator. Figure 1 shows the experimental setup. For a high-impedance, low-current accelerator, the space-charge limiting current in the interacting zone must be minimized. A 1.5 kA, 400 keV electron beam was focused by a short magnetic lens to form a virtual cathode approximately 4 mm in diameter. The microwave radiation generated is in the wavelength range of 6.2 - 11.5 mm (frequency range of 26-58GHz) and the peak power is approximately 1 MW. The frequency spectrum of the virtual cathode microwave radiation is relatively wide. This is due to the strong non-linear interaction between the electron beam and the microwave. Furthermore, the drift tube is not selective to the mode and frequency of the microwave because it is a multi-mode and broad bandwidth device. In order to enhance the emission efficiency, a specially designed experimental structure will be used to create a multi-stage virtual cathode in future work. A schematic diagram of the multi-vircator concept is shown in the paper.

X-Ray Laser Gain Measurements, Beam Optics Diagnostics in Ne-Like Ge

91FE0401B Beijing WULI XUEBAO [ACTA PHYSICA SINICA] in Chinese Vol 39, No 11, Nov 90 pp 1745-1750 [MS Received 21 May 90]

[Article by He Shaotang [0149 4801 1016], He An [0149 1344], Chunyu Shutai [3196 0060 2579 3141] and Shen Huazhong [3088 5478 1813] of Southwest Institute of Nuclear Physics and Chemistry, Chengdu: "X-Ray Laser Gain Measurements, Beam Optics Diagnostics in Ne-Like Ge"]

[Abstract] The X-ray laser gain of the 3s-3p transition in Ne-like Ge is studied on the Shen Guang laser facility, which is a high-power (10^{12} W) Nd pulsed laser. Its wavelength is 1.06 μm and its pulse width is 1.2 ns. The output energy per pulse is 550 - 650 J. As shown in Figure 2, the light is focused into a line approximately 20 mm wide and 180 μm long by a number of cylindrical lenses. 1-mm-thick Ne-like Ge targets from 7 - 18 mm in length are used. A 1-m-radius-of-curvature compact grazing incidence spectrograph was installed perpendicular to the incident laser beam to measure the gains of the X-ray lasing lines over a wavelength range of 2 - 32 nm. The grating has 1200 lines/mm and the resolution is 0.005 nm. The gain coefficients corresponding to the 19.638, 23.224, 23.627, 24.743 and 28.643 nm lasing lines were found to be 3.06, 3.99, 3.72, 2.36 and 4.59 cm^{-1}, respectively. These numbers are in excellent agreement with earlier results obtained at NRL (Naval

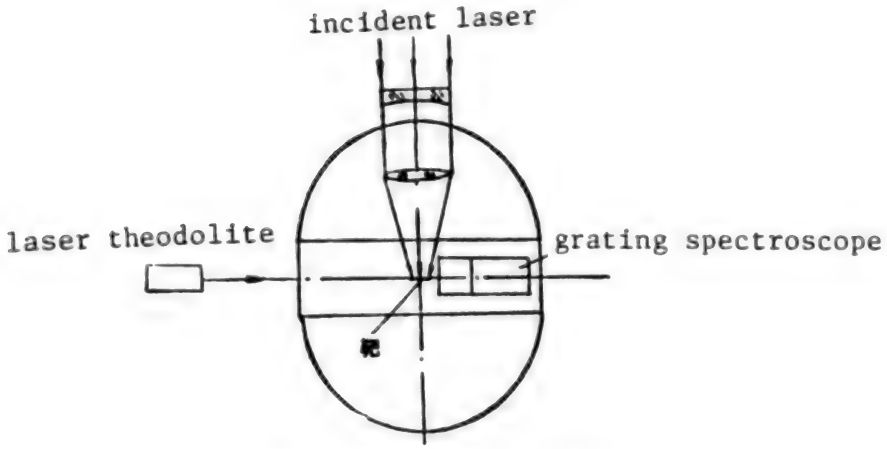

Figure 2. Experimental Apparatus

Research Laboratory). The dependence of laser transition intensity on the target surface pumping power density was also investigated. When the pumping power density is below 7 x 10^{12} W/cm^2, there is no X-ray lasing because not enough Ne-like ions are produced. As power goes up, the concentration of Ne-like ions increases and the intensity of the lasing line also becomes stronger. However, after the power density reaches a certain level, excessive ionization causes the concentration of Ne-like ions to fall and the lasing line intensity also drops. An optimum target surface power density was not found on the Shen Guang laser facility.

The transmission characteristics of the X-ray laser were also investigated. Compared to other spontaneous lines in the UV X-ray spectra of Ge, the 3s-3p lines of Ne-like Ge are short and narrow. Furthermore, each line has a non-uniform intensity distribution along the non-dispersion direction which is characteristic of X-ray laser transmission in a linear plasma. The divergence angles of these X-ray lasing lines are around 12 mrad. The off-axis angles are about 5.7 mrad.

Designing Large Digital Sonar System Using Cascade Link Array Processors

91FE0185A Beijing SHENGXUE XUEBAO [ACTA ACUSTICA SINICA] in Chinese Vol 15, No 3, May 90 pp 230-237 [MS Received 24 Jan 89]

[Article by Liu Qiushi [0491 4428 1395], Li Shicai [2621 1102 2088], Li Qihu [2621 0796 5706] and Sun Zhen [1327 1073] of the Institute of Acoustics of the Chinese Academy of Sciences: "Technique for Designing Large Digital Sonar System Using Cascade Link Array Processors"]

[Text] Abstract: From the analysis of the characteristics of sonar signal processing, a new architecture using cascade link array processors is proposed. Various elements of the structure, including data bus protocol, data transmission and basic processing cell are described in detail. Finally, a procedure to design a digital sonar using cascade link array processors is presented.

I. Introduction

With the development of VLSI technology and digital signal processors, it is technically feasible to design sonar with a multi-processor architecture.[1-3] Compared to a digital sonar with extensive hardware, a multi-processor sonar is more flexible, lower in cost and requires a shorter design cycle. Therefore, hardware-loaded digital sonars will be obsolete soon. A multi-processor sonar has the following advantages: 1. Different processing requirements (such as wave formation, delay estimation, adaptive noise rejection, etc.) can be handled by processors of essentially identical hardware design. 2. The same hardware can be shared by several algorithms to finish the same processing requirement in order to deal with different situations. 3. The processing functions are distributed to different processors so that the data flow path and failure detection become localized. Consequently, the design complexity is reduced and reliability is improved. Conventional processor-based sonars employ the standard micro-processor bus link and standard signal processing cell architecture. When the amount of data exceeds a certain level, dispatch of data becomes a big problem. In the process of mapping an algorithm to a processing cell, it happens quite often that the algorithm cannot fit in the pre-designed processing cell and the algorithm has to be broken up into pieces. Thus, a large amount of intermediate results will have to be transmitted on the main bus or the pre-designed dual RAM channels. Due to limited frequency bandwidth of the bus, a bottleneck will occur. This undesirable effect exists because there is no way to build a sonar with a multi-processor design. To this end, this paper describes the method and technology of designing a real time multi-processor sonar using cascade link array processors. The technology includes: 1. mapping of digital signal processing flowchart onto a cascade link array structure, 2. establishment of the linking structure, 3. categorization of the linking structures, 4. mapping of

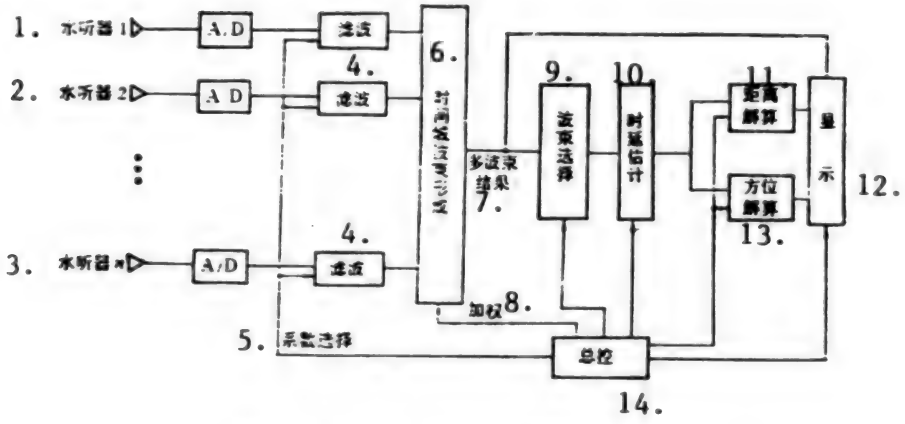

Figure 1. Passive Orientation/Range Sonar

Key: 1. hydrophone 1 2. hydrophone 2 3. hydrophone 3 4.filter 5. index selection 6.time domain wave formation 7. multiple wave result 8. weighted 9. wave selection 10. time delay estimation 11. distance determination 12. display 13. orientation determination 14. bus control

two levels of linking structure to the standard processing cell, and 5. configuration of master control and selection of master control command cell. The standard cell designs for different linking structures are also given in this paper.

II. Analysis of Data Flow in Sonar

A sonar processes the raw data step by step and transforms it into the final result. From the overall function, the results of calculation done in the earlier stage is input into the next stage to be further processed until the desired result is obtained. This is the so-called cascade method. At any processing stage, data must be processed continuously in sequence according to the time of arrival. In order to obtain spatial gain, an array of transducers (hydrophones) is used. Therefore, there are several identical channels at different processing stages. Figure 1 shows the block diagram of a passive orientation/range detection sonar station.

From the figure the multi-channel hydrophone signals are converted by A/D converters and filtered before forming a time domain wave pattern to be displayed on a screen. The master control selects a split beams of a wave signal to perform a generalized estimation of delay time. Finally, the orientation angle and range are determined and shown on the display. Therefore, this sonar can be considered as a five-stage cascade system: i.e. filtering, beam formation, spectrum analysis, orientation and range determination, and display.

The unique features associated with sonar signal processing such as the presence of identical channels and the cascade structure make the cascade link array structure to be discussed later very suitable for a multi-processor sonar system.

III. Analysis of the Cascade Structure

Although we have not seen published results concerning distributing the computation requirements of a sonar according to the arrangement shown in Figure 2, however, similar studies have been in other fields such as the famous Systolic Wavefront method.[4] We will propose a mapping method similar to the Wavefront method by taking the special characteristics of sonar signal processing into account in a separate paper. The emphasis here is placed on the link. Once the computation of sonar signal processing is reasonably distributed into the cascade structure shown in Figure 2, then the key issue is how to complete the link between two stages.

There are five different linking structures. 1. Single-Out Single-In, i.e. the output of a processing cell is the input of the other, denoted as SOSI. 2. Multiple-Out Single-In, i.e. the output of several processing cells is the input of another processing cell, denoted as MOSI. 3. Single-Out Multiple-In, i.e. the output of a single processing cell is the input of several cells, denoted as SOMI. 4. Multiple-Out Single-Select, i.e. one of the outputs of several processing cells is chosen as the input of another cell, denoted as MOSS. 5. Multiple-Out Multiple-In, i.e. the output of several processing cells is used as the input for a number of cells, denoted as MOMI. Figure 3 shows the above five types of linkage. In reality, MOSS is a form of MOSI. However, from the standpoint of a sonar system, the amount of processing decreases from front to back. Hence, a trapezoidal structure with a large front end and a small back end requires the least amount of equipment. Therefore, MOSS is often employed in a cascade link array system and is singled out as a linkage mode. SOSI is equivalent to MOSI or SOMI with l=1. It is possible to use the data transmission method for MOSI or SOMI.

MOSI (Figure 3(b)) has only two data transmission methods. (1) Active receiving cell, or converging method. Cells at the k level such as P_{kj1}, P_{kj2}, P_{kj3},..., P_{kjl} prepare the data and notify P_{k+1j} to pick it up. It is easy to figure out that it only requires a single bus to pick up

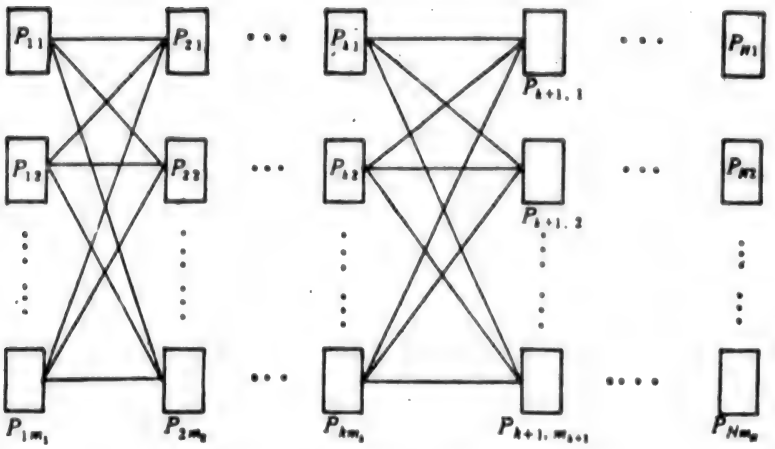

Figure 2. The Usual Cascade Architecture

(a) SOSI

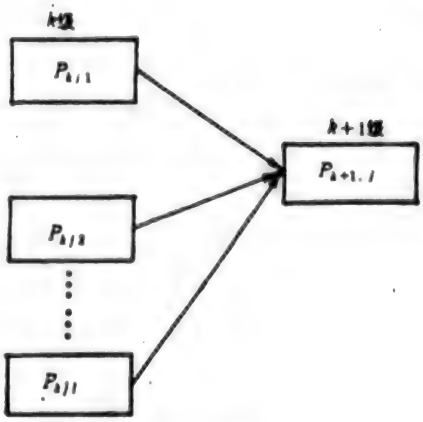

(b) MOSI

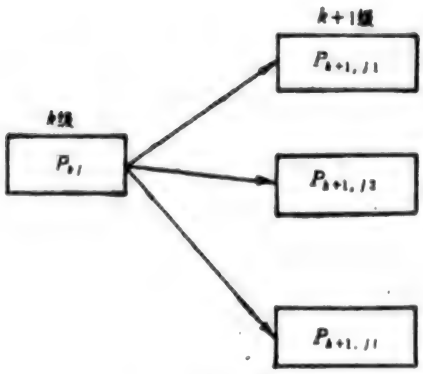

(c) SOMI

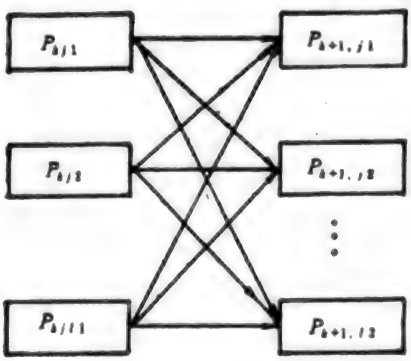

(d) MOMI

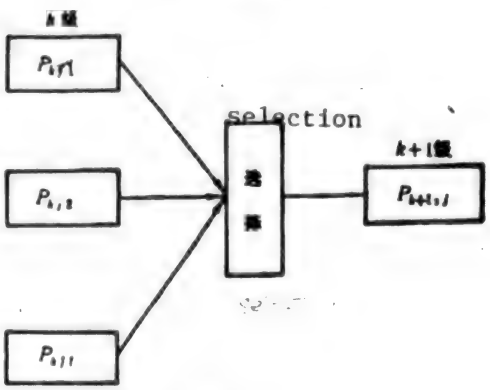

(e) MOSS

Figure 3. Different Linkage Structures

the data for cells P_{kj1}, P_{kj2}, P_{kj3},..., P_{kjl} that have identical structure and perform the same operation. Let us assume that N numbers are to be picked up from each transmitting cell, then a receiving cell needs l N τ to pick up the numbers. τ is the time required to pick up a number, which is dependent upon the bandwidth of the bus. (2) Active transmitting cell mode, or broadcasting method. Cells at the k level prepare the data and simultaneously transmit to cell P_{k+1j} at the k+1 level. In this case, P_{k+1j} is required to have l independent address common reception registers and l data bus lines. Although the time required for the data to be completed is only N τ in the broadcasting mode, the price to pay is to use l transmitting cells to transmit data. Therefore, if time permits, to the extent possible MOSI data transmission should be done using the converging method. There are also two data transmission methods associated with the SOMI linking structure, as shown in Figure 3(c). 1. Converging method. This method requires each transmitting cell have l independent RAM addresses to store identical results to allow l receiving cells P_{k+1j1}, P_{k+1j2}, ...P_{k+1jl} to simultaneously pick up the data from l bus lines. If there is only one data bus, then it is necessary to introduce a synchronous control mechanism among P_{k+1j1}, P_{k+1j2}, ...P_{k+1jl} to permit time sharing. Then, the control is spread to the entire system which makes it more complicated. Therefore, it is not rational to use the converging method for data transmission in a SOMI structure. 2. Broadcasting method. P_{kj} is capable of transmitting the result simultaneously to P_{k+1j1}, P_{k+1j2}, ...P_{k+1jl} through a single data bus within a period of N τ. MOSS is used when one of the results from the cells in the earlier stage is chosen as the input for a cell in the next stage. Therefore, its data transmission can be handled by the converging method with a MOSI linkage structure. In this case, it is necessary to install an identification device on the transmitting cell. The receiving cell transmits an identification code to determine whether the RAM should operate or not.

MOMI is the most complex structure among the five structures. Other than the display stage, it not used in any sonar systems for land, submarine, torpedo, and ship use. Nevertheless, for completeness in theory, we use a fixed linkage network to handle the data transmission for this structure. From the viewpoint of a receiving cell, it has to receive different processed results from different types of cells at different times. Then, these results are

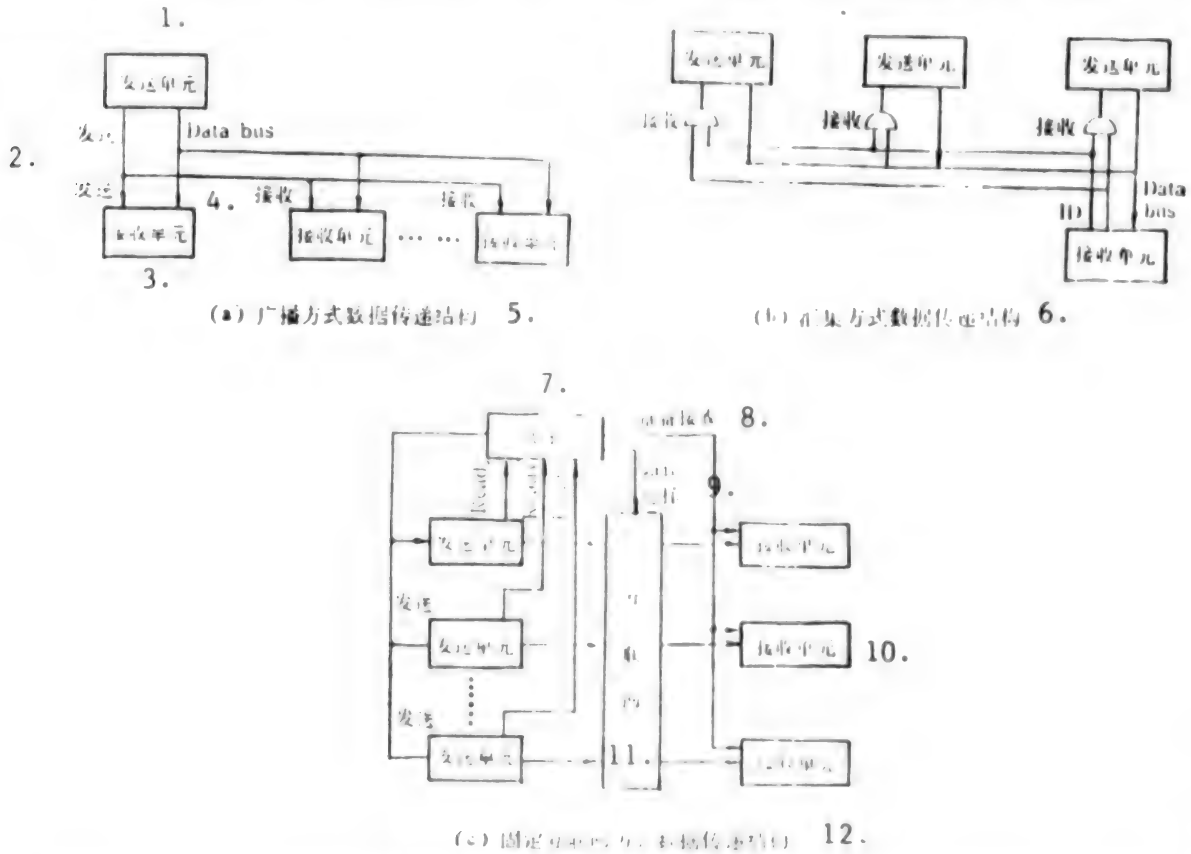

Figure 4. Data Transmission Structures

Key: 1.transmitting cell 2. transmit 3. receiving cell 4. receive 5. broadcasting data transmission structure 6. converging data transmission structure 7. master control 8. ready to receive 9. channel selection 10. receiving cell 11. linkage network 12. fixed linkage network data transmission structure

consolidated as the input for the computer. Hence, a master control programmed multi-channel switch can meet this requirement.

IV. Master Control for the Cascade Link Array Sonar

In the development of large data processing systems, control components such as the command controller in a computer and the progress adjustment program in an operating system usually play a dominant role. Although a system using a control component as the core unit is more flexible, however, it is difficult to design. It is often the most complicated part of the system. Using the cascade structure proposed in this paper, almost all the data flow is completed between two stages. The master control no longer has to deal with complicated data and program dispatch. Instead, it only has to program commands for the cascade link array for data processing. Therefore, the design complexity is significantly reduced. In a cascade link array structure, there are many cells of identical function. In order to directly issue a command to each processing cell, the bus must have tremendous driving power. Furthermore, each cell must have a register to receive commands. We can select the least number of identical cells on the same level as the cells to receive commands. Through the link bus, they are transmitted to cells that actually execute the commands. As long as the maximum delay between issuance and execution can satisfy the system requirement and software control is acceptable, the design can be simplified. For example, the data transmission structure for SOMI is

d_1	d_2	$\cdots$	d_N

Moreover, receiving cells $P_{k+1,1}$, $P_{k+1,2}$, ...$P_{k+1,l}$ are required to receive command e. If each receiving cell receives command e directly, it requires a command bus and l receiving registers. Let us install a register on $P_{k,j}$ to receive command e, then the data transmitting structure becomes

e	d_1	d_2	$\cdots$	d_N

Then, it is possible to transmit command e to the RAM of each receiving cell via the data bus. As a matter of fact, it is more appropriate to change the command or sonar function from front to back. For instance, a multi-purpose active/passive sonar may have to specify the location of the target by the noise location method. It is then switched to active precision tracking after it approaches the target. Thus, when a command propagates from front to back, it arrives at the corresponding processing cell in a timely manner to alter the operating mode of the sonar. The switch-over time can be reduced.

V. Designing the Processing Cell

A processing cell in a cascade link array system has three assignments: i.e. pick up data from the previous stage, compute and output to the next stage. Figure 5 shows the cell input, output structures in different linkage modes. Based on these basic structures, a processing cell can be designed from the linkage structure and the data transmission equation. Figure 6 shows the logic diagram of a complete processing cell whose input stage has a SOMI linkage structure in broadcasting mode and output stage is a converging MOSI structure.

VI. Design Procedure for Cascade Link Array Processors

From previous sections, the hardware and software configuration can be designed based a sonar data processing flowchart using cascade link array processors. The method can be summarized into the following six steps: 1) Map the algorithm onto the cascade structure based on the computation load. 2) Specify the linkage mode between two stages. 3) determine the data transmission method. 4) Determine command receiving cells based on response speed and arrival conditions. 5) Design data transmission format and command transmission format. 6) Design cell hardware and software and master control software. The results of each step in these six steps can satisfy the design requirements in previous steps. Therefore, as long as the original signal processing function design can meet the original objective, the final hardware and software must be able to satisfy the overall requirements.

References

[1] Knight, W. C., et al., "Digital Signal Processing for Sonar," REV. IEEE., 69, 1981, pp 1451-1506.

[2] Bartram, I. F., et al., "Fifth Generation Digital Sonar Processing," IEEE TRANS., OE-2, 1977, pp 337-343.

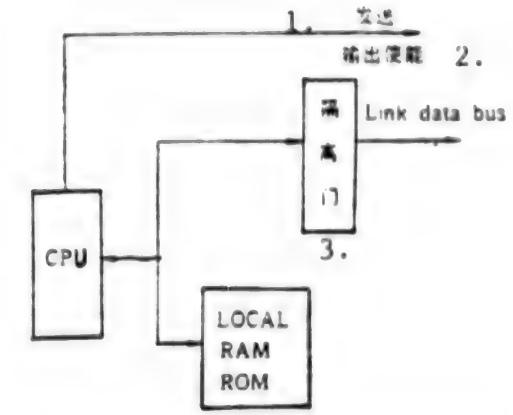

6. (a) SOMI 按广播方式传送数据的输出结构

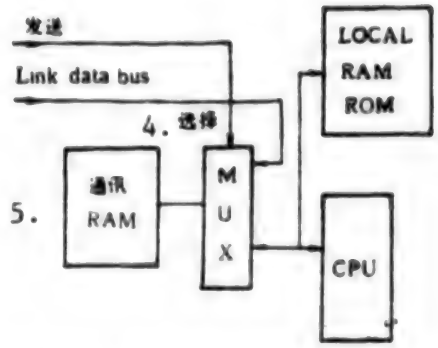

7. (b) SOMI 按广播方式传送数据的输入结构

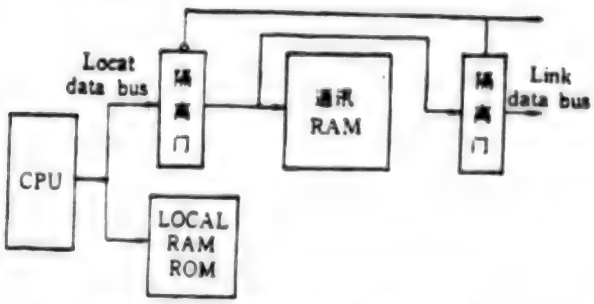

9. (c) MOSI 按汇聚方式传送数据的输出结构

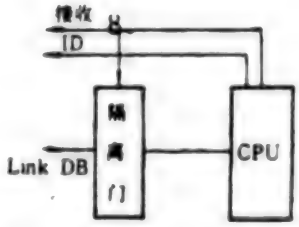

10. (d) MOSI 按汇聚方式传送数据的输入结构

Figure 5. Bus Configurations Associated With Different Data Transmission Modes

Key:1. transmit 2. enable output 3. isolation gate 4. selection 5. communication RAM 6. SOMI data transmission output structure in broadcasting mode 7. SOMI data transmission input structure in broadcasting mode 8. receive 9. MOSI data transmission output structure in converging mode 10. MOSI data transmission input structure in converging mode

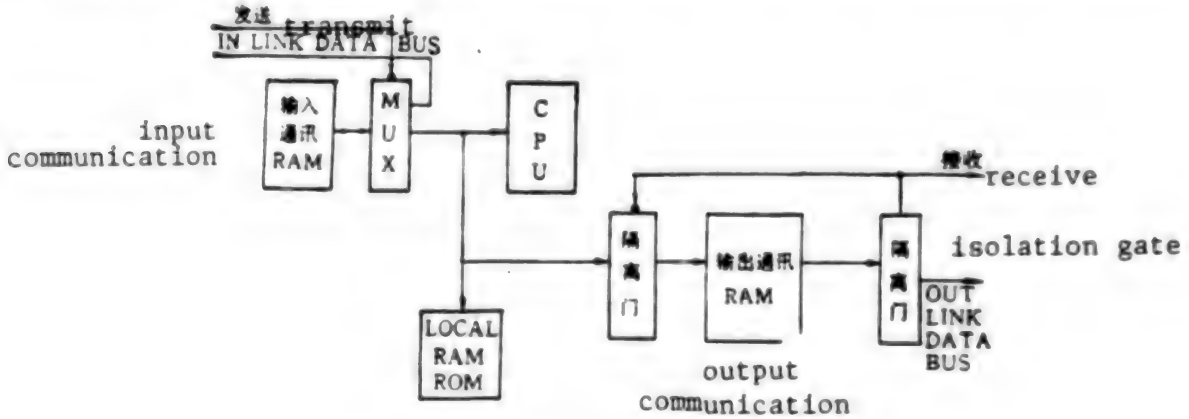

Figure 6. A Complete Cell Structure

[3] Whitehouse, H. J., et al., "Linear Signal Processing Architecture," Aspects of Signal Processing, Lierdal Publishing, 1977.

[4] Kung, S. Y., "VLSI Array Processors," Prentice Hall, 1987.

Pulsed Slab Nd:YAG Laser

91FE0426A Shanghai ZHONGGUO JIGUANG [CHINESE JOURNAL OF LASERS] in Chinese Vol 18 No 1, Jan 91 pp 1-4 [MS received 5 Apr 90]

[Article by Gong Mali [7255 7456 3810], Han Kai [7281 0418], Xu Shaolin [1776 4801 2651], and Zhai Gang [5049 0474] of the Southwest Institute of Technical Physics, Chengdu: "Pulsed Slab Nd:YAG Laser"]

[Text] **Abstract**

A 124 x 12 x 6 mm^3 pulsed slab Nd:YAG laser has been developed. The free oscillation single-pulse output is 24 J and the overall efficiency is 2.5 percent. The electro-optic Q-switched laser output is 860 mJ/pulse and the pulse width is 12-15 ns. The switching efficiency is 72 percent.

Key words: slab laser, YAG laser

Using a slab structure is an effective way to obtain high-power output from a solid-st. laser. Its unique point is that light propagates along a saw-tooth-shaped path in the laser medium. This technique simultaneously pumps the medium and cools down its surface. Consequently, this a.proach effectively overcomes thermal deformation of the medium and its effect on the output power and the quality of the beam, and enables the device to produce a high-quality, high-power output. The slab design was originally presented by W. S. Martin et al. Detailed theoretical and experimental studies were done by scientists at Stanford University and GE. It has become one of the active research areas in lasers. Moving media, diode pumping and various solid-state slab lasers have been developed. The mean power output of solid-state slab laser is of the order of 1,000 watts.[1]

In this work, preliminary experiments were done with a pulsed slab Nd:YAG at a repetitive operating frequency. In addition, end-face loss of the slab laser was analyzed.

I. Design and Structure

Figure 1 shows the end structure of the slab Nd:YAG laser. In order to obtain a more uniform pumping face, a multi-planar reflective focusing cavity is usually used to excite the medium along one direction.[2] However, the pumping efficiency of this kind of cavity is low. We are using a more efficient silver-plated double ellipsoid cavity. By properly designing the cavity and selecting the pumping light parameters, uniform pumping was achieved. When the two pumping lamps are placed at the two outside focal points of the double ellipse, the conjugate images coincide at the common focus (i.e., inner focal points). The pumping lamp is considered to discharge uniformly in the discharge region. Therefore, by properly choosing the cavity parameters and pumping lamp diameter, it is possible to put the slab medium in the elliptical conjugate image (Figure 2) to obtain a relatively uniform pumping effect. When the slab is 2t thick and 2w wide, the eccentricity of the cavity e and the pumping lamp diameter d_L required to achieve uniform pumping can be determined by the following equations:

$$d_L = 2\sqrt{2}\, t\, \frac{1-e^2}{1-e^2} \tag{1}$$

$$\frac{(1+e^2)^2(1-e^2)^2}{[1-e)^4-(1+e^2)^2]\left(\operatorname{arctg}\frac{\omega}{t}\right)^2-(1+e^2)^2} = \frac{4(t^2-\omega^2)}{d_L^2} \tag{2}$$

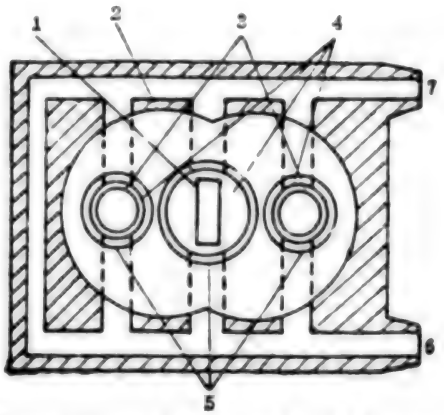

Figure 1. Cross Section of the Slab Laser

Key: 1.YAG slab crystal; 2. focusing cavity; 3. pumping lamp; 4. cooling water; 5. quartz water-cooled jacket; 6. cooling water inlet; 7. cooling water outlet

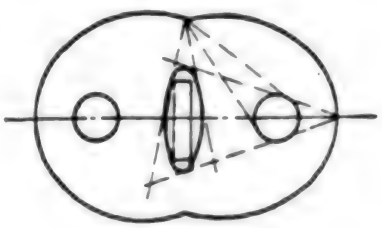

Figure 2. Slab in the Elliptical Focusing Cavity

The size of the cavity is determined by the diameter of the pumping lamp, thickness and width of the slab, and cooling requirement. Usually, in a multi-plane reflective focusing cavity, it is more desirable to use an insulating material or a material with thermal conductivity identical to that of the slab to hold the sides of the slab in order to obtain uniform face pumping and face cooling to minimize thermal deformation.[3] In our device, in order to ensure a high pumping efficiency, the sides were

not held by another material. Instead, the entire slab is cooled, including the sides. This is to compensate for the pumping on the sides to overcome thermal deformation along that direction. There is a one-dimensional thermal gradient in the slab along the thickness direction.

II. End-Face Loss

In a solid-state slab laser, oblique incidence is the usual mode of coupling between the light beam and the excitation medium. This method does not require the aid of any coupling prisms. It is simple in structure, which makes it easy for multiple-lamp pumping from both sides and water cooling. The end-face angle can be carefully designed to reduce end-face loss, or to obtain highly polarized laser output.

In solid-state slab lasers, the larger the angle of incidence is (60° to 70°), the higher reflective loss at the end-face becomes. Furthermore, the long excitation medium also makes it more difficult to coat the end-face with an anti-reflective film. The reflective loss at the end-face is shown in Figure 3. For S-polarized light and natural polarized light, reflective loss decreases as the end-face angle θ increases (as shown in curves a and b in the figure). For P-polarized light, when the end-face angle θ is close to the Brewster angle, the loss is minimal. However, the structure of the device would be complicated by cutting the end-face angle of the slab to the Brewster angle.[4] On the other hand, if light propagates along a zigzag path in the slab, the effective gain length is increased. Nevertheless, with increasing end-face angle θ, the effective gain length is reduced. Therefore, both reflective loss and effective gain length must be taken into consideration in the selection of a suitable end-face angle. We believe that it is more appropriate to use 36-40° for the YAG slab.

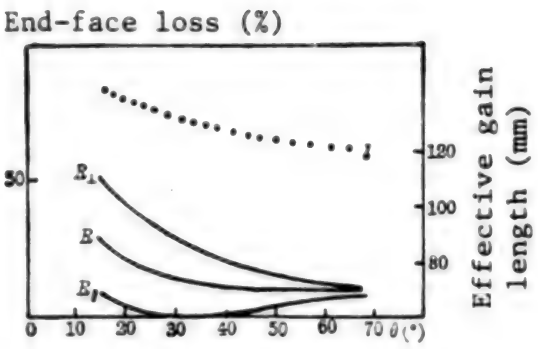

Figure 3. End-Face Loss vs. Effective Gain Length

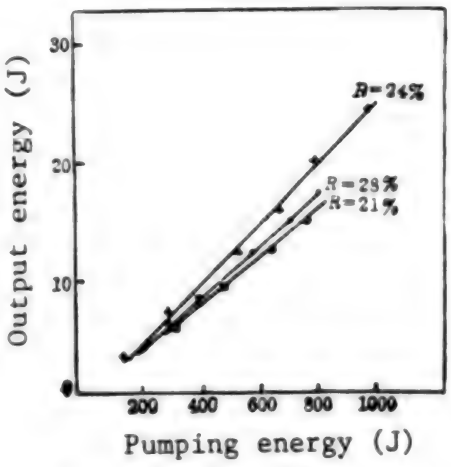

Figure 4. Free-Oscillation Pulse Output

III. Output Characteristics

Figure 4 shows the free-oscillation output characteristics of the slab YAG laser. The optimal output reflectance is 24 percent. In this case, the threshold of the device is 50 J, the maximum monopulse energy output is 24 J, the oblique efficiency is 2.5 percent, and the pulse width is 0.4 ms. At 28 and 21 percent output mirror reflectance, the oblique efficiencies are 2.2 and 2.0 percent, respectively. The divergence angle along the width direction was experimentally determined to be approximately 0.18 mrad. This is close to the diffraction limit and indicates that this total cooling method can effectively eliminate the effect of side pumping.

Figure 5 shows the huge Q-switched laser pulse output. By properly adjusting the delay time of Q-switching, a very high switching efficiency can be obtained. The maximum switching efficiency is 72 percent with stability. In this case, the Q-switched pulse output increases linearly with the pumping input. The maximum Q-switched pulse energy is 860 mJ and the pulse width is 12-15 ns. Although the Q-switched pulse energy is raised further when the pumping energy is increased beyond this point, the pulse then widens and several pulses emerge. Figure 6 shows the stability of Q-switching. The switch developed works well and maintains a stable efficiency. The efficiency fluctuates less than 10 percent. At lower switching efficiencies, the stability is further improved to better than 5 percent.

A solid-state slab laser is more advantageous for repetitive high-frequency, high-mean-output operation. To this end, we conducted a preliminary study and the results are shown in Figure 7. The free-oscillation repetition frequency is 70 Hz, the mean power output is 49 W, and the overall efficiency is 1 percent. Compared to a single pulse, it fell. The reason is that the charging energy was reduced when the power supply was switched to operate at the repetition frequency. The maximum pumping energy per pulse is only 70 J, just slightly above the threshold of the device. During Q-switching, the repetition frequency is 50 Hz and the mean Q-switched power output is 20 W.

Li Junshu [2621 0319 2579], Wu Dazhi [0702 1129 1807], and Yu Shufan [0060 3219 0416] also participated in this work.

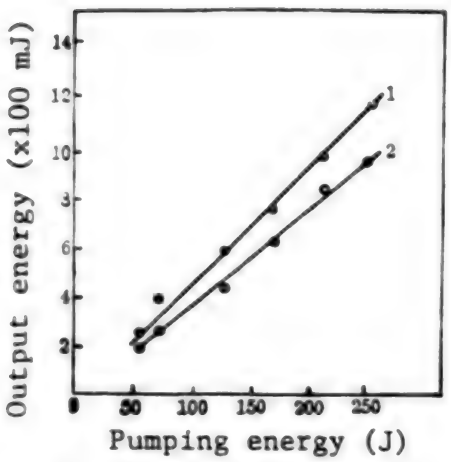

Figure 5. Q-Switched Pulse Output

Key: 1. free oscillation; 2. Q-switched

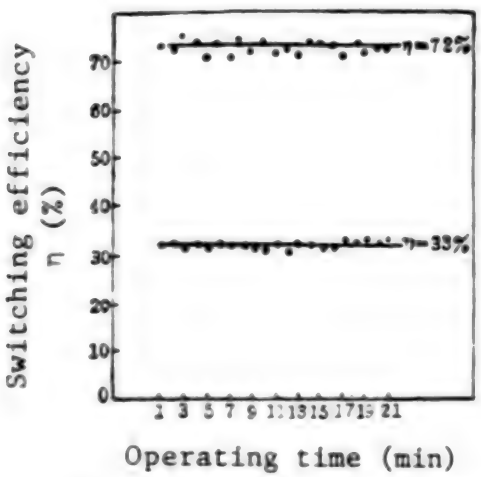

Figure 6. Stability of Q-Switching

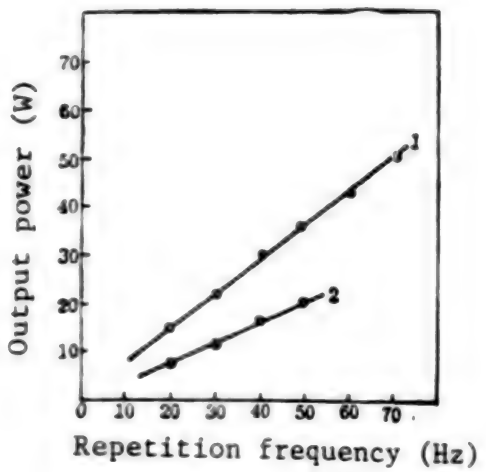

Figure 7. Mean Power Characteristics

Key: 1. free oscillation; 2. Q-switching

New CCD Image-Pickup Camera Developed

91P60168A Beijing ZHONGGUO DIANZI BAO [CHINA ELECTRONICS NEWS] in Chinese 1 Mar 91 p 3

[Article by Yu Ruming [0151 3067 2494]: "Institute 44 Unveils Low-Light CCD Image-Pickup Camera"]

[Summary] The model GS8290 LLCCD [low-light charge-coupled device] image-pickup camera recently developed by MMEI's Institute 44 has applications in military night vision, public security monitoring, medicine, biology, optics, and robot vision. This camera, which employs enhanced CCD image sensors, includes an optical-waveguide-fiber board which tightly couples the CCD image sensors to the image intensifier. The camera has about 360,000 pixels in a 604 (H) x 588 (W) array with a light-sensing surface area of 14 (H) x 10.5 (W) square meters [sic; apparently a typo for centimeters or millimeters]; SNR is better than 46 dB and electronic shutter speed is adjustable from 1/60 to 1/2000 second.

Evolution From Periodicity to Non-Periodicity of Electron Phase Orbits in Free-Electron Laser with Untapered Wiggler

91FE0401A Beijing WULI XUEBAO [ACTA PHYSICA SINICA] in Chinese Vol 39, No 11, Nov 90 pp 1745-1750 [MS Received 23 Jan 90]

[Article by Zhang Shichang [1728 0013 2490], Hu Zhongxiu [5170 1813 4423] and Wang Wenyao [3769 2429 5096] of the Dept. of Physics, Univ. of Electronic Science and Technology of China, Chengdu: "Evolution From Periodicity to Non-Periodicity of Electron Phase Orbits in Free-Electron Laser With Untapered Wiggler"]

[Abstract] There have been numerous theoretical and experimental studies on free electron laser as a high

References

1. C. L. M. Ireland, LASER FOCUS, Vol 24, No 11, 1988, p 49.

2. Ding Liming [0002 7787 2494], et al., ZHONGGUO JIGUANG [CHINESE JOURNAL OF LASERS], Vol 16, No 6, 1989, p 423.

3. G. F. Albrecht, et al., IEEE J. QUANT. ELECTR., Vol QE-22, No 11, 1986, p 2099.

4. Wang Rongrui [3769 2051 3843], JIGUANG YU HONGWEI [LASERS AND INFRARED], Vol 18, No 12, 1988, p 9.

5. J. M. Eggleston, et al., IEEE J. QUANT. ELECTR., Vol QE-20, No 3, 1984, p 289.

power tunable coherent light source. However, the randomness of electron motion has not been investigated in depth. It is known that the motion of electrons becomes random when the amplitude of the wiggler increases. If the spatial variation rate of the wave number of the wiggler varies significantly, a portion of the electron orbit becomes non-periodic and random. Furthermore, the motion of electrons is random when sideband instability becomes substantial. In most theoretical analyses, the energy transfer between the electron beam and the optical field is considered to be negligible. In reality, energy is transferred from the electron beam to the optical field so that radiation is amplified upon excitation. Therefore, it is meaningful to consider the amplitude of the optical field as a variable. In this work, a one-dimensional model is employed. Based on Kroll-Morton-Rosenbluth theory, the wiggler is assumed to be circularly polarized. The electron phase orbit can be divided into two categories depending upon the initial conditions: i.e. trapped electrons and untrapped electrons. Transition of trapped electrons from periodicity to non-periodicity is possible as long as there is sufficient time for interaction. The control parameter may be the amplitude of the wiggler, rate of spatial wave number variation, intensity or sideband instability, or plasma frequency.

Threshold Conditions for Pulsed Laser-Induced Spallation in Metals

91FE0193B Chengdu QIANG JIGUANG YU LIZI SHU [HIGH POWER LASER AND PARTICLE BEAMS] in Chinese Vol 2, No 3, Aug 90 pp 345-352

[Article by Sun Chengwei [1327 2110 4885] and Zhuang Shiming [8369 0099 2494] of Southwest Institute of Fluid Physics: "Threshold Conditions for Pulsed Laser-Induced Spallation in Metals"; MS received 25 May 90, revised 15 Jun 90]

[Abstract] The threshold conditions for the spallation in metal targets due to reflection of stress wave induced by a laser pulse, including the relation between laser flux and stress wave intensity, the attenuation of the propagating stress wave, and interaction between incident and reflected wave, are considered in this paper. An approximation of the attenuation and expansion of the one-dimensional plane stress wave induced by laser is obtained based on a simplified theoretical model. The results can be summarized as follows: (1) At a specific laser flux and target thickness spallation occurs only when the laser pulse is within a certain range. The lowest laser flux threshold corresponds to the optimum pulse width, i.e. d is approximately b/2. (2) Numerical calculation shows that spallation occurs when the laser flux is at least 10^{11} W/cm^2 and energy is of the order of 10^{3}J/cm^2 even without taking two-dimensional effect into consideration. Although the flux requirement may be reduced with a longer pulse, however, it cannot be used with a thin target because it burns through the target. (3) The direct heating effect of the laser and the impact of the stress wave will affect the intrinsic structure and fracture conditions of the target such as thermal activation of micro-defect and thermal softening of the material. However, if the laser pulse interaction is short and the spallation is near the back interface, then only impact heating needs to be considered. When the pressure is above 10 GPa, thermal softening effect can be neglected. (4) Since the laser effect and mechanical issues are separately discussed in this model, the method and conclusions are also applicable to flyer impact induced spallation.

Numerical Simulations of Laser Ignition of PETN and Interactions of Explosion Waves with Al Targets

91FE0193C Chengdu QIANG JIGUANG YU LIZI SHU [HIGH POWER LASER AND PARTICLE BEAMS] in Chinese Vol 2, No 3, Aug 90 pp 359-365

[Article by Zhang Zhongzheng [1728 1813 3791], Duan Zhuping [3088 4376 1627], Liu Xiaoping [0491 1420 5393] and Sun Chengwei [1327 2110 4885] of Southwest Institute of Fluid Physics (first and last authors) and Institute of Mechanics of the Chinese Academy of Sciences (second and third authors): "Numerical Simulations of Laser Ignition of PETN and Interactions of Explosion Waves with Al Targets"; MS received 11 Jul 90]

[Abstract] Laser ignition of the high explosive PETN is simulated using a one-dimensional fluid dynamics program SSS. The effects of laser waveform and window thickness are discussed. An elastic plastic fluid model is employed and Hook's law and Von Mises yield condition are obeyed. Furthermore, the Kennecly melting model is used. Spallation is treated by a stress gradient and artificial viscosity is of the PIC type. In addition, it is assumed that the explosive obeys Arrhenius law. Since the laser pulse intensity is below the GW level, it is assumed that the absorption follows the Bouguer-Lambert-Beer law.

A comparison of the results of this work to other experimental and calculated data indicates that this model appears to be reasonable. In addition, the following conclusions can be reached: (1) Within the power density range of interest, i.e. 10^6 - 10^8 W/cm^2, the most important mechanism between the explosive and laser is thermal. (2) Ignition will be affected by laser waveform and laser-explosive coupling. (3) Within a certain range, ignition threshold decreases with increasing window thickness. Ignition is not possible without a window. When the window is relatively thin and the laser power density is close to its critical value, ignition takes place inside the explosive, instead of on its surface. Thermal expansion of the explosive is one of the major factors of laser energy loss. Thermal conduction may be neglected. (4) Ignition threshold can be lowered by adding an aluminum film of the proper thickness between the window and the explosive.

Four Devices Developed by MMEI's Institute 16 Pass Technical Appraisal

91P60163A Hefei DIWEN YU CHAODAO [CRYOGENICS AND SUPERCONDUCTIVITY] in Chinese Vol 19 No 1, Feb 91 pp 71-72

[Article by Wang Huizhi [3769 1979 5347]: "MMEI's Research Institute 16 Holds Technical Appraisal Conference"; see earlier report in JPRS-CST-91-004, 5 Feb 91 p 28]

[Summary] At a technical appraisal conference held in Hefei 21-22 October 1990, four devices developed by MMEI's Institute 16 were formally accredited by a panel of 10 technical experts from nine institutions. The four are a "high-Tc-superconductor Suo-er-wen [?Solvay] refrigerator," a "high-Tc-superconductor non-magnetic refrigerator," a "high-sensitivity underwater target detector/superconducting quantum interferometer [or SQUID]," and a "high-Tc-superconductor microwave resonant cavity."

The high-Tc-superconductor Suo-er-wen refrigerator is a closed-loop continuous cryocooler with a 23K-300K operating temperature range, a refrigerating output of 21W/77K, a cool-down time of 18 minutes to 77K, and a power consumption of 1.455 kW. The technical experts noted that, in terms of refrigerating output and minimum temperature, this device meets 1980's international standards for comparable products.

The high-Tc-superconductor non-magnetic refrigerator is a functional cooling source for high-Tc superconducting devices. Applications include weak-magnetic-field detection, aerial mineral prospecting, anti-submarine detection, and medical treatment. Minimum operating temperature is 46K, refrigerating output is 0.209W/77.35K, input power is less than 180W, weight is 14 kg, and the number of stages is two. The experts noted that the device's refrigerating output easily surpasses the value of 100 mW at 77K required for operation of a high-Tc SQUID.

The high-sensitivity underwater target detector/high-Tc SQUID, which operates at 77K (liquid-N temperature), replaces SQUIDs which operate at liquid-He temperature. This device has applications in magnetic anomaly detection, low-frequency communications, anti-submarine detection, and precision-measurement instruments used in medical treatment and other scientific areas. The device has a flux resolution of 5.1×10^{-4} $\varphi_0/Hz^{1/2}$ [where φ_0 (the magnetic flux quantum) = 2.07×10^{-7} gauss-m^2] in the 0-100 Hz range and an energy resolution of 2.8×10^{-27} J/Hz. The device can withstand numerous recyclings between 77K and 300K [i.e., room temperature].

With its high Q value, the $YBa_2Cu_3O_{7-x}$ high-Tc-superconductor microwave resonant cavity is an extremely useful passive microwave device that can serve as a frequency-stabilized oscillator or as a two-stage frequency standard. At 10 GHz in the TE_{011} mode, the superconducting cavity has a no-load quality factor Q_0 of 9.2×10^4 at a 56K temperature.

Influence of Coupling Network on Noise, Frequency Response of DC SQUID Magnetometer

91P60161A Hefei DIWEN YU CHAODAO [CRYOGENICS AND SUPERCONDUCTIVITY] in Chinese Vol 19 No 1, Feb 91 pp 57-64

[Article by Zhang Lihua [1728 0448 5478], Weng Yaojun [5040 1031 6874], and Chen Lie [7115 3525] of the Chinese Academy of Sciences, Institute of Physics, Beijing: "Influence of Coupling Network on Noise and Frequency Response of DC SQUID Magnetometer"; MS received 25 Aug 90, revised 22 Oct 90]

[Abstract] The use of an RLC-circuit resonant transformer as the coupling network between a DC SQUID input and the preamplifier of a DC SQUID magnetometer is reported, and the effects of the resonant transformer's transfer ratio and Q value on magnetometer performance are described. After impedance-matching, the noise figure of the preamplifier is 2.3 dB and the network Q value is 2.5, enabling the magnetometer to have a high slew rate and wide frequency response. A SQUID simulator is improved and used to fabricate an experimental apparatus.

Results of the simulation as well as testing of the experimental apparatus (shown in Figure 1 below) are as follows: in the fast operating mode, system frequency response (3 dB bandwidth) was measured at 3.5 kHz for the simulator and 3 kHz for the experimental system; in the slow operating mode, the values were 600 Hz and 900 Hz, respectively. Slew rate SR_{max} (the maximum rate of change in magnetic sensitivity to avoid amplifier distortion) in the fast operating mode measured 2.5×10^4 φ_0/s [φ_0 (the magnetic flux quantum) is about 2.07×10^{-7} gauss-m^2] for the simulator and 3.0×10^4 φ_0/s for the experimental system; in the slow operating mode, the measured values were 1.0×10^3 φ_0/s and 8.9×10^2 φ_0/s, respectively. When system noise (rms value of equivalent flux noise φ_N) was 3.5×10^{-5} $\varphi_0/Hz^{1/2}$, 4.8×10^{-4} $\varphi_0/Hz^{1/2}$, and 3.0×10^{-3} $\varphi_0/Hz^{1/2}$, corresponding measured values of slew rate were 1.5×10^4 φ_0/s, 1.3×10^4 φ_0/s, and 7.0×10^3 φ_0/s, respectively.

References

1. J. Clarke, W. M. Goubau, and M. B. Ketchen, J. LOW TEMP. PHYS., 25, 99 (1976).

2. Frederick Wellatood, C. Heiden, and John Clarke, REV. SCI. INSTRUM., 55, 952 (1984).

3. Jukka Knuutila, Seppo Ahlfors, et al., REV. SCI. INSTRUM., 58, 2146 (1987).

4. Qiu Jingwu and Chen Kaiyuan, DIWEN YU CHAODAO [CRYOGENICS AND SUPERCONDUCTIVITY], 14 (3), 40 (1986).

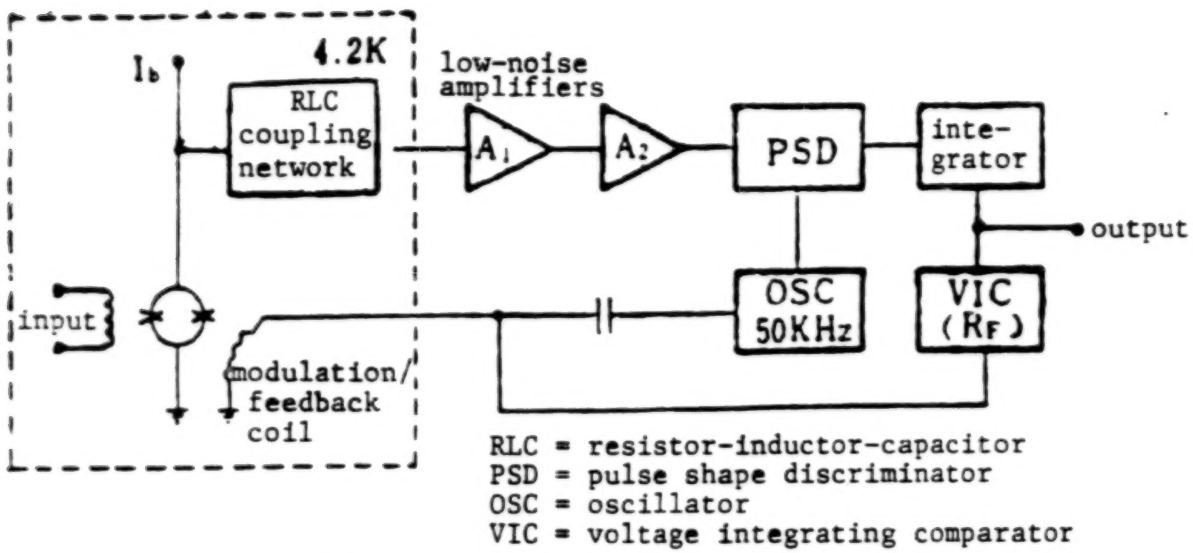

Figure 1. Schematic Diagram of DC SQUID Magnetometer

5. V. V. Danilov, K. K. Likharev, et al., IEEE TRANS. ON MAGN., MAG-13, 240 (1977).

6. Yang Peiran, Chen Lie, et al., DIWEN YU CHAODAO [CRYOGENICS AND SUPERCONDUCTIVITY], 17 (1), 21 (1989).

7. C. D. Matchebacher and F. C. Fitchen, "Low-Noise Electronic Design," John & Sons, Inc. (1973).

Effect of Doping Ag on Superconducting Properties of TlBaCaCuO System

40100046 Beijing GUISUANYAN XUEBAO [JOURNAL OF THE CHINESE CERAMIC SOCIETY] in Chinese Vol 19 No 1, Feb 91 pp 69-74

[English abstract of article by Li Chengen, Zhao Meiyu, Wu Wenjun, et al. of the Shanghai Institute of Ceramics, CAS. (MS received 25 Jun 90)]

[Text] Effect of doping Ag on superconducting properties of superconductors of TlBaCaCuO system has been studied. The experimental results show that as the amount of Ag doped is not more than 0.3mol, it is advantageous for the formation of the 2223 phase. By properly raising the quantity of Tl or Cu in the composition at the time of doping, the sintering temperature of the samples can be reduced; superconductors of TlBaCaCuO system with T_{co} = 122K and T_{onset} = 136K can be also obtained.

Key words: TlBaCaCuO system; doping Ag; superconductors; 2223 phase

Optimum Percentage of Pb and Appropriate Thermal Procedure for Preparation of 110K $Bi_{2-x}Pb_xSr_2Ca_2Cu_3O_y$ Superconductor

40100041A Hefei DIWEN YU CHAODAO [CRYOGENICS AND SUPERCONDUCTIVITY] in Chinese Vol 19 No 1, Feb 91 pp 17-20

[English abstract of article by Wan Fabao, Ping Yimei, and Fan Jiangshui of Northwestern University; MS received 22 Aug 90]

[Text] High-Tc superconductors of the $Bi_{2-x}Pb_xSr_2Ca_2Cu_3O_y$ system have been synthesised by a solid-state reaction method and the role of Bi/Pb substitution has been studied extensively using electrical resistivity and X-ray diffraction. It was found that the best results were obtained for x = 0.3 and that a one-step sintering process is necessary for a better control of the thermal process. A SQUID [superconducting quantum interference device] working at 77K was built from Bi-based material and its curve was observed.

rf-SQUID and the Grain Property of YBCO

40100041B Hefei DIWEN YU CHAODAO [CRYOGENICS AND SUPERCONDUCTIVITY] in Chinese Vol 19 No 1, Feb 91 pp 40-44

[English abstract of article by Lin Dong, Yang Tao, et al. of the Department of Physics, Northwest University; Li Jianping, Wang Jingrong, and Wu Xiaozu of the Research Institute of Nonferrous Metals, Baoji; and Zhang Chaoxing and Zhang Hongbin of the Hefei Research Institute of Cryogenics and Electronic Technology; MS received 4 Oct 90]

[Text] The preparation of a YBCO [77K-operating-temperature] rf-SQUID, the characteristics of V_{rf}-φ_e, and the properties of the material have been

studied. The reason why the necked size of the device is far larger than the coherence length of the material has been discussed. It is believed that if the grain property of high-T_c superconductors can be understood correctly and utilized rationally, some requirements of excellent devices with high-T_c materials which are prepared by general solid-state reaction techniques can be satisfied.

In-Situ Deposition of YBCO Superconducting Thin Films by Laser Ablation

40100041C Hefei DIWEN YU CHAODAO [CRYOGENICS AND SUPERCONDUCTIVITY] in Chinese Vol 19 No 1, Feb 91 pp 45-48

[English abstract of article by Zhang Yaogang, Shi Changqing, and Fan Shoushan of the Department of Physics, Qinghua University; MS received 3 Oct 90, revised 10 Nov 90]

[Text] Initial research on in-situ fabrication of high-T_c superconducting thin films is presented. The YBCO films with zero-resistance temperature T_c (R = 0) > 84K have been successfully fabricated by a pulsed laser deposition technique with substrate temperature at about 600°C. The target used is sintered $YBa_2Cu_3O_x$ bulk disk. The substrate material is $SrTiO_3$ (100) single crystal. The in-situ thin film, black in color, shows a smooth surface with thickness about 1,500 Angstroms. The XRD and SEM results show that the films are orientated with C-axis perpendicular to film surface. In a zero magnetic field, the critical current density J_c (77.5K) > 5×10^5 A/cm^2.

END OF FICHE

DATE FILMED

4 June 1991